# We are IntechOpen, the world's leading publisher of Open Access books Built by scientists, for scientists

## 6,900
Open access books available

## 186,000
International authors and editors

## 200M
Downloads

Our authors are among the

## 154
Countries delivered to

## TOP 1%
most cited scientists

## 12.2%
Contributors from top 500 universities

CLARIVATE ANALYTICS
**BOOK CITATION INDEX**
INDEXED

**WEB OF SCIENCE**™

Selection of our books indexed in the Book Citation Index in Web of Science™ Core Collection (BKCI)

## Interested in publishing with us?
Contact book.department@intechopen.com

# Sliding Mode Control for Industrial Controllers

Khalifa Al-Hosani[1], Vadim Utkin[2] and Andrey Malinin[3]
*[1,2]The Ohio State University,*
*[3]IKOR*
*USA*

## 1. Introduction

This chapter presents sliding mode approach for controlling DC-DC power converters implementing proportional integral derivative (PID) controllers commonly used in industry. The core design idea implies enforcing sliding mode such that the output converter voltage contains proportional, integral and derivative components with the pre-selected coefficients. Traditionally, the method of pulse width modulation (PWM) is used to obtain a desired continuous output function with a discrete control command. In PWM, an external high frequency signal is used to modulate a low frequency desired function to be tracked. However, it seems unjustified to ignore the binary nature of the switching device (with ON/OFF as the only possible operation mode) in these power converters. Instead, sliding mode control utilizes the discrete nature of the power converters to full extent by using state feedback to set up directly the desired closed loop response in time domain. The most notable attribute in using sliding mode control is the low sensitivity to disturbances and parameter variations (Utkin, Guldner, & Shi, 2009), since uncertainty conditions are common for such control systems. An irritating problem when using sliding mode control however is the presence of finite amplitude and frequency oscillations called chattering (Utkin, Guldner, & Shi, 2009). In this chapter, the chattering suppression idea is based on utilizing harmonic cancellation in the so-called multiphase power converter structure. Moreover, the method is demonstrated in details for the design of two main types of DC-DC converter, namely the step-down buck and step-up boost converters.

Control of DC-DC step-down buck converters is a conventional problem discussed in many power electronics and control textbooks (Mohan, Undeland, & Robbins, 2003; Bose, 2006). However, the difficulty of the control problem presented in this chapter stems from the fact that the parameters of the buck converter such as the inductance and capacitance are unknown and the error output voltage is the only information available to the designer. The problem is approached by first designing a switching function to implement sliding mode with a desired output function. Chattering is then reduced through the use of multiphase power converter structure discussed later in the chapter. The proposed methodology is intended for different types of buck converters with apriory unknown parameters. Therefore the method of observer design is developed for estimation of state vector components and parameters simultaneously. The design is then confirmed by means of computer simulations.

The second type of DC-DC converter dealt with in this chapter is the step-up boost converter. It is generally desired that a sliding mode control be designed such that the output voltage tracks a reference input. The straightforward way of choosing the sliding surface is to use the output voltage error in what is called direct sliding mode control. This methodology leads to ideal tracking should sliding mode be enforced. However, as it will be shown, direct sliding mode control results in unstable zero dynamics confirming a non-minimum phase tracking nature of the formulated control problem. Thus, an indirect sliding mode control is proposed such that the inductor current tracks a reference current that is calculated to yield the desired value of the output voltage. Similar to the case of buck converters, chattering is reduced using multiphase structure in the sliding mode controlled boost converter. The results are also confirmed by means of computer simulations.

## 2. Modeling of single phase DC-DC buck converter

The buck converter is classified as a "chopper" circuit where the output voltage $v_C$ is a scaled version of the source voltage $E$ by a scalar smaller than unity. The ideal switch representation of a single-phase buck converter with resistive load is shown in Fig. 1. Simple applications of Kirchhoff's current and voltage laws for each resulting circuit topology from the two possible ideal switch's positions allow us to get the system of differential equations governing the dynamics of the buck converter as it is done in many control and power electronics textbooks. We first define a switch's position binary function $u$ such that $u = 1$ when the ideal switch is positioned such that the end of the inductor is connected to the positive terminal of the input voltage source and $u = 0$ otherwise. With this, we get the following *unified* dynamical system:

$$\frac{di_L}{dt} = \frac{1}{L}\left(uE - v_C\right) \tag{1}$$

$$\frac{dv_C}{dt} = \frac{1}{C}\left(i_L - \frac{v_C}{R}\right) \tag{2}$$

Most often, the control objective is to regulate the output voltage $v_C$ of the buck converter towards a desired average output voltage equilibrium value $v_{sp}$. In many applications, power converters are used as actuators for control system. Also, the dynamics of the power converters is much faster than that of the system to be controlled. Thus, it might be reasonable to assume that the desired output voltage $v_{sp}$ is constant. By applying a discontinuous feedback control law $u \in \{0,1\}$, we command the position of the ideal switch in reference to an average value $u_{avg}$. Depending on the control algorithm, $u_{avg}$ might take a constant value as in the case of Pulse Width Modulation PWM (referred to as duty ratio) or a time varying value as in the case of Sliding Mode Control SMC (referred to as equivalent control $u_{eq}$). In both cases (constant, or time varying), the average control $u_{avg}$ takes values in the compact interval of the real line [0,1].

Generally, it is desired to relate the average value of state variables with the corresponding average value of the control input $u_{avg}$. This is essential in understanding the main *static* features of the buck converter. In steady state equilibrium, the time derivatives of the average current and voltage are set to zero and the average control input adopts a value

given by $u_{avg}$. With this in mind, the following steady-state equilibrium average current and voltage are obtained:

$$\overline{v}_C = u_{avg}E \tag{3}$$

$$\overline{i}_L = \frac{\overline{v}_C}{R} = \frac{u_{avg}E}{R} \tag{4}$$

According to equation (3) and given the fact that the average control input $u_{avg}$ is restricted to the interval [0,1], the output voltage $v_C$ is a fraction of the input voltage $E$ and the converter can't amplify it.
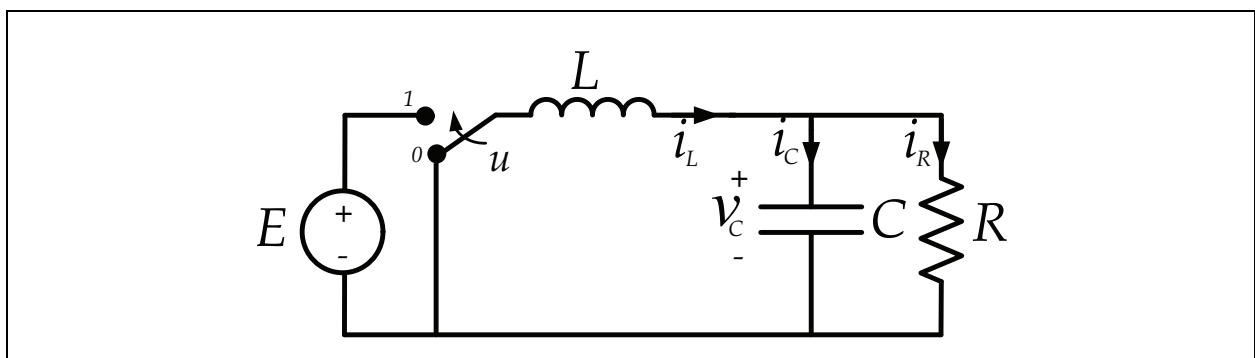


Fig. 1. Ideal switch representation of a single phase DC-DC Buck converter.

## 3. Sliding mode control of single phase DC-DC Buck converter

Control problems related to DC-DC converters are discussed in many textbooks. The control techniques used in these textbooks differ based on the problem formulation (e.g. available measured state variables as well as known and unknown parameters). PWM techniques are traditionally used to approach such problems. In PWM, low-power signal is amplified in average but in sliding mode, motion in some manifold with desired properties is enforced by discontinuous control. Moreover, sliding mode control provides a better solution over PWM due to the binary nature of sliding mode fitting the discrete nature of the available switches in modern power converters. In this section, the problem of regulating the output voltage $v_c$ of a DC-DC buck converter towards a desired average output voltage $v_{sp}$ is presented.

Consider the DC-DC buck converter shown in fig. 1. A control law $u$ is to be designed such that the output voltage across the capacitor/resistive load $v_C$ converges to a desired unknown constant reference voltage $v_{sp}$ at a desired rate of convergence. The control $u$ is to be designed under the following set of assumptions:

- The value of inductance $L$ and Capacitance $C$ are unknown, but their product $m = 1/LC$ is known.
- The load resistance $R$ is unknown.
- The input voltage $E$ is assumed to be constant floating in the range $[E_{min}, E_{max}]$.
- The only measurement available is that of the error voltage $e = v_C - v_{sp}$.
- The current flowing through the resistive load $i_R$ is assumed to be constant.

The complexity of this problem stems from the fact that the voltage error $e = v_C - v_{sp}$ and constant $m$ is the only piece of information available to the controller designer.

The dynamics of the DC-DC buck converter shown in fig. 1 are described by the *unified* dynamical system model in equations (1-2). For the case of constant load current i.e. $i_R \approx$ constant , the model can be reduced to that given by equations (6-7) by introducing new variable $i$ :

$$i = \frac{1}{C}\left(i_L - i_R\right) = \frac{1}{C}\left(i_L - \frac{v_C}{R}\right) \tag{5}$$

$$\frac{di}{dt} = \frac{1}{LC}\left(uE - v_C\right) = m\left(uE - v_C\right) \tag{6}$$

$$\frac{dv_C}{dt} = i \tag{7}$$

Note that the model described by equations (6-7) is only valid when the load resistance is constant and thus, the load current at steady state is constant. Alternatively, the load current $i_R$ might be controlled through an independent controller such that it's always constant. For the case of changing load resistance, the model given by equations (6-7) becomes inaccurate and the converter must instead be modeled by equations (1-2) or equations (8-9) using the change of variable given by equation (5).

$$\frac{di}{dt} = m\left(uE - v_C\right) - \frac{1}{RC}i \tag{8}$$

$$\frac{dv_C}{dt} = i \tag{9}$$

A conventional method to approach this problem ($v_C$ to track $v_{sp}$) is to design a PID controller with the voltage error $e = v_C - v_{sp}$ being the input to the controller. Here, a sliding mode approach to implement a PID controller is presented (Al-Hosani, Malinin, & Utkin, 2009). A block diagram of the controller is shown in Fig. 2. The dynamics of the controller is described by equations (10-11) where $L_1$ and $L_2$ are design constants properly chosen to provide stability (as will be shown later).

$$\frac{d\tilde{v}}{dt} = L_1\left(v_C - v_{sp}\right) \tag{10}$$

$$\frac{d\tilde{i}}{dt} = m\left[u - \tilde{v} + L_2\left(v_C - v_{sp}\right)\right] \tag{11}$$

Sliding mode is to be enforced on the PID-like switching surface given by:

$$s = \frac{v_C - v_{sp}}{c\sqrt{m}} + \frac{\tilde{i}}{m} = 0 \tag{12}$$

where $c$ is a constant parameter that is selected by the designer to provide desired system's characteristics when sliding mode is enforced. The control law based on this surface is given by:

$$u = \frac{1}{2}\left(1 - sign(s)\right) = \begin{cases} 0 & \text{if } s < 0 \\ 1 & \text{if } s < 0 \end{cases} \tag{13}$$
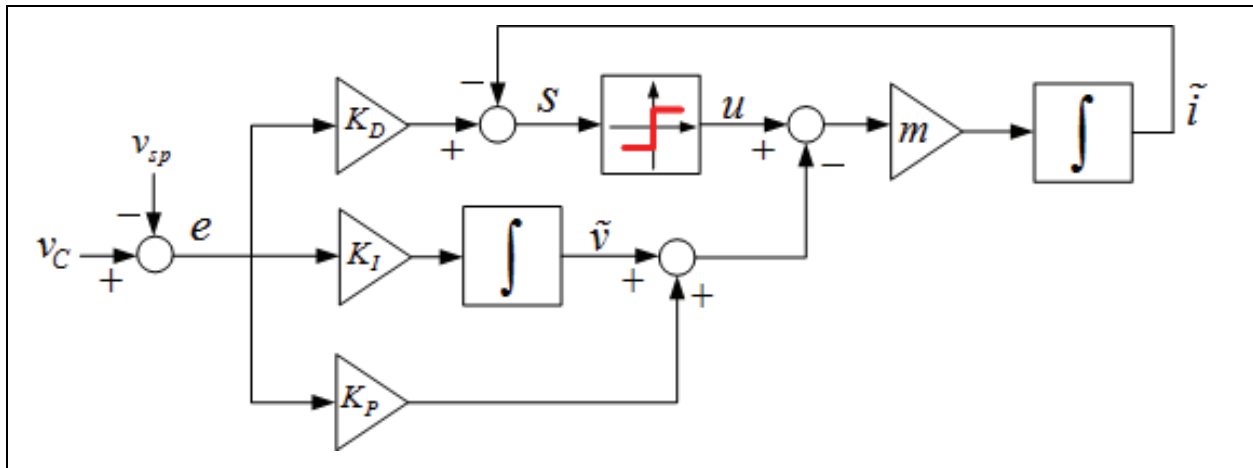


Fig. 2. Sliding Mode implementation of PID Controller.

For sliding mode to exist, the condition $s\dot{s} < 0$ must be always satisfied. Using the equivalent control method, the solution to equations $s = 0$ and $\dot{s} = 0$ must be substituted in equations (6-7) to get the motion equation after sliding mode is enforced along the switching plane $s = 0$ in the system's state space, thus

$$s = 0 \Rightarrow \tilde{i} = -\frac{\sqrt{m}}{c}\left(v_C - v_{sp}\right) \tag{14}$$

$$\dot{s} = 0 \Rightarrow u_{eq} = -L_2\left(v_C - v_{sp}\right) + L_1\int\left(v_C - v_{sp}\right)dt - \frac{1}{c\sqrt{m}}\dot{v}_C \tag{15}$$

As evident from equation (15), the equivalent control $u_{eq}$ is indeed equivalent to a PID controller (Fig. 2) with respectively proportional, derivative, and integral gains $K_P = -L_2$, $K_I = L_1$, and $K_D = -1/c\sqrt{m}$. The equivalent control $u_{eq}$ in (15) is then substituted into equations (6-7) and (10-11) resulting in the following 3rd order system equations:

$$\frac{d^2 v_C}{dt^2} = m\left[E\tilde{v} - \frac{E}{c\sqrt{m}}\frac{dv_C}{dt} - EL_2\left(v_C - v_{sp}\right) - v_C\right] \tag{16}$$

$$\frac{d\tilde{v}}{dt} = L_1\left(v_C - v_{sp}\right) \tag{17}$$

To analyze stability, we write the characteristic equation of the close loop system.

$$\lambda^3 + \frac{E\sqrt{m}}{c}\lambda^2 + m\left(EL_2 + 1\right)\lambda - mEL_1 = 0 \tag{18}$$

The constant parameters $L_1$, $L_2$, and $c$ are chosen to provide stability of the system, i.e

$$c > 0, \quad EL_2 + 1 > 0, \quad L_1 < 0 \quad \frac{\sqrt{m}}{c}\left(EL_2 + 1\right) > -L_1 \tag{19}$$

Satisfying the above conditions will provide stability and the system will have the following equilibrium point:

$$v_c = v_{sp}, \quad \dot{v}_c = i = 0, \quad \mathrm{E}\tilde{v} = v_{sp}. \tag{20}$$

Fig. 3 shows simulation of the system with parameters $C = 10\,\mu F$, $L = 2\,\mu H$, $c = 0.0045$, $L_1 = -10^4$, and $L_2 = 199.92$. The switching device is implemented using a hysteresis loop set such that the switching frequency is controlled to be about 100 KHz. As evident from fig. 3, the output voltage $v_C$ converges (with finite amplitude oscillation or chattering) to the desired reference voltage $v_{sp}$ at a rate set by the chosen controller's parameters.
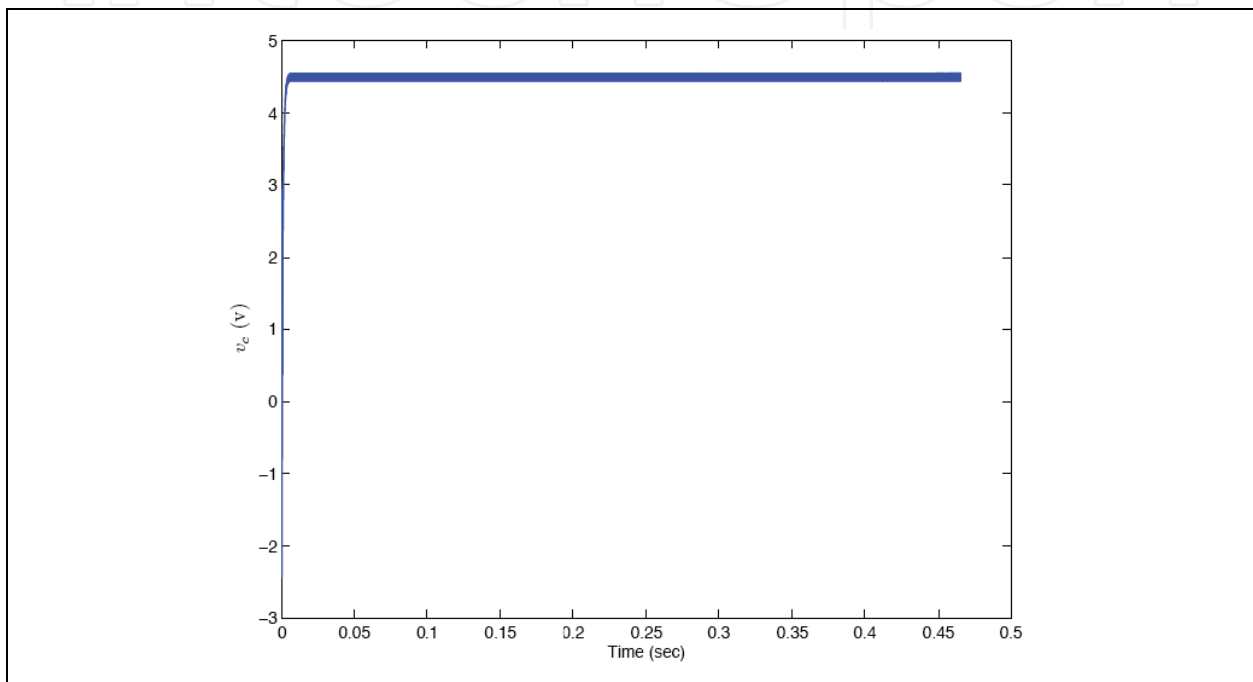


Fig. 3. Sliding mode PID control of single-phase buck converter.

## 4. Estimation in sliding mode PID controlled single phase DC-DC buck converter

The sliding mode PID controller described by equations (10-13) assumes only the knowledge of the parameter $m$ and the voltage error measurement $e = v_C - v_{sp}$. However, the parameter $m$ might be unknown or varying from one converter to another. Hence, the problem is to complement the sliding mode PID controller with a parameter estimator such that the controller's parameter can be selected automatically. For this, two types of observers are presented next (Al-Hosani, Malinin, & Utkin, 2009). The first type is a sliding mode observer, which assumes that both the reference voltage $v_{sp}$, and the voltage error $e = v_C - v_{sp}$ are known. On the other hand, the second type is an asymptotic observer that assumes that the voltage error $e = v_C - v_{sp}$ measurement is the only piece of information available.

A. *Sliding Mode Observer*

The converter's parameter $m$ is assumed to be unknown in this case. Thus, we initially feed the sliding mode PID controller described by equations (10-13) with a guess value of $m_0$. In

addition, both the voltage error $e = v_C - v_{sp}$ and the desired set point voltage $v_{sp}$ are assumed to known. Defining the known function $G = Eu - v_C = Eu - e - v_{sp}$, equations (6-7) can be rewritten as:

$$\frac{di}{dt} = mG \tag{21}$$

$$\frac{dv_C}{dt} = i \tag{22}$$

The following sliding mode observer is now proposed:

$$\frac{d\hat{i}}{dt} = \hat{m}G \tag{23}$$

$$\frac{d\hat{m}}{dt} = -M \operatorname{sign}\left(G\bar{i}\right) \tag{24}$$

where $\hat{m}$ is the estimate of converter parameter $m$, and $\hat{i}$ is the estimate of variable $i$ with mismatch $\bar{i} = \hat{i} - i$. Choosing the constant $M > m$ will enforce sliding mode along the sliding surface $\bar{i} = 0$, and the average value (easily obtained using a low pass filter) of $\hat{m}$ will tend to $m$. The only restriction in this observer design is that estimation should be fast enough (such that the real value of the estimated parameters is reached before $G = 0$). To overcome this problem, we introduce the following modification to equation (24):

$$\frac{d\hat{m}}{dt} = \begin{cases} -M \operatorname{sign}\left(G\bar{i}\right) & \text{if} \quad |e| \geq \Delta \\ 0^* & \text{if} \quad |e| < \Delta \end{cases} \quad \text{* in discrete time implementation} \tag{25}$$

$$\hat{m}_{k+1} = \hat{m}_k \text{ for } |e| < \Delta$$

The sliding mode observer described by equations (23) and (25) needs knowledge of the error derivative $i = de/dt$ which is not measured. A straightforward solution is to employ a first order filter with the voltage error $e = v_C - v_{sp}$ being the input and the output replacing the error derivative in equation (25). Several computer simulations are performed to confirm the operation of proposed observer. Fig. 4 shows simulation 1 result when using the following set of parameters: $L = 0.81\mu H$, $C = 0.6\mu F$, $v_{sp} = 8V$, $E = 12V$, $c = 1 \times 10^{-5}$, $L_1 = -1 \times 10^4$, $L_2 = 200$. For Simulation 2 shown in Fig. 5, the following set of parameters is used: $L = 0.5\mu H$, $C = 1.7\mu F$, $v_{sp} = 8V$, $E = 12V$, $c = 1 \times 10^{-5}$, $L_1 = -1 \times 10^4$, $L_2 = 200$. For Simulation 3 shown in Fig. 6, the following set of parameters is used: $L = 0.22\mu H$, $C = 0.76\mu F$, $v_{sp} = 8V$, $E = 12V$, $c = 1 \times 10^{-5}$, $L_1 = -1 \times 10^4$, $L_2 = 200$. As evident from these three different simulations, $\hat{m}_{eq}$ (average value of $\hat{m}$) converges to the real value of $m$ with a desired rate of convergence set the observer parameters. The simulations also show that the estimation process was fast enough (estimation was complete before the average value of $G$ reaches zero).
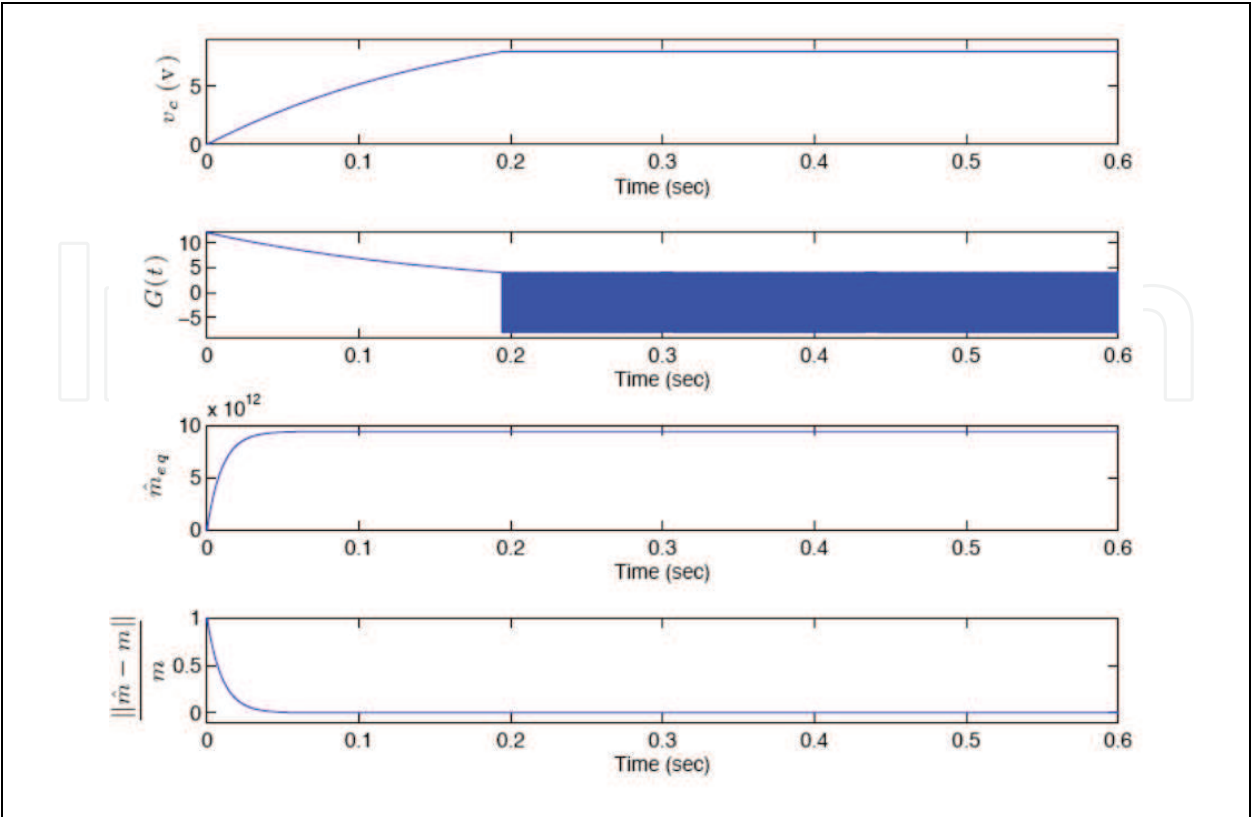
Fig. 4. Simulation 1 SM PID Control of DC-DC buck converter with SM observer.
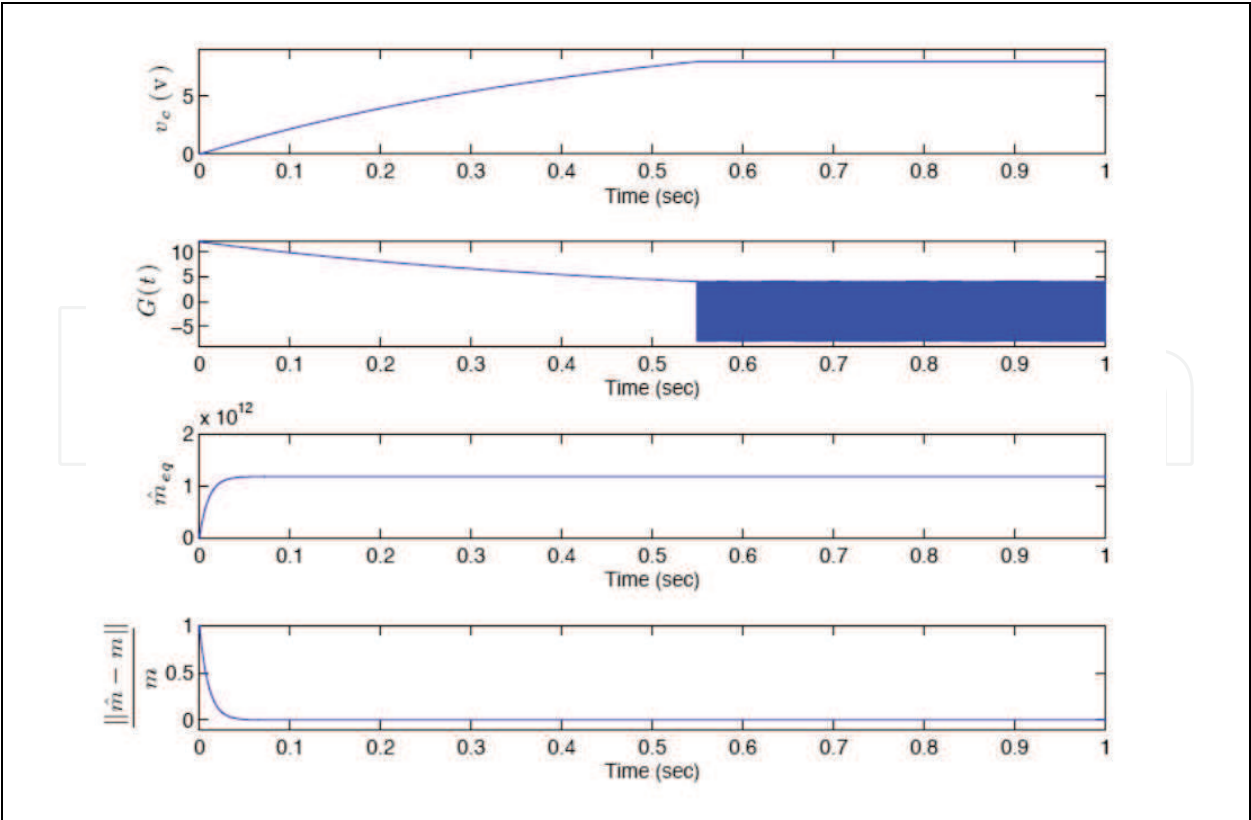


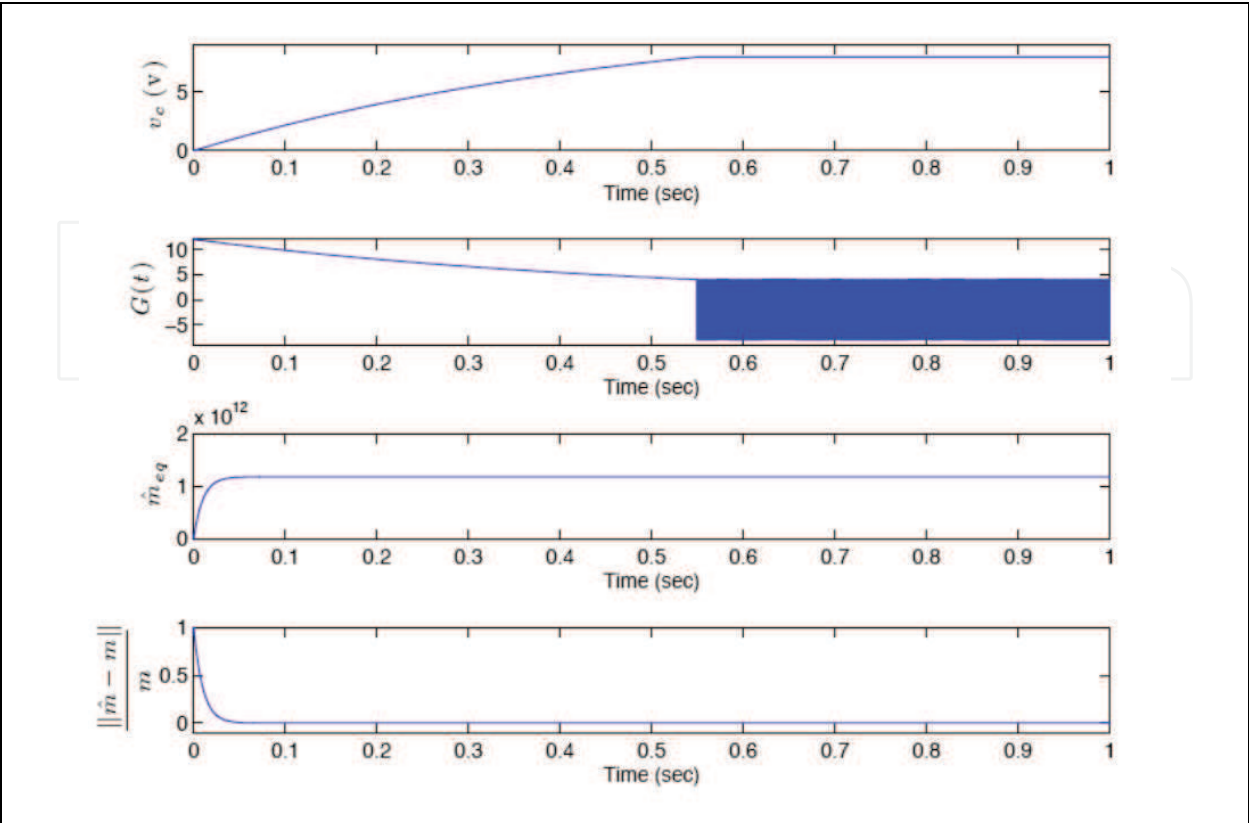Fig. 5. Simulation 2 SM PID Control of DC-DC buck converter with SM observer.

Fig. 6. Simulation 3 SM PID Control of DC-DC buck converter with SM observer.

B. *Asymptotic Observer*

In designing this observer, it is assumed that both the converter's parameter $m$ and the reference set point voltage $v_{sp}$ are unknown. Thus, an asymptotic observer with both parameters being simultaneously estimated is proposed. We first define $G = Eu - v_C = Eu - e - v_{sp} = \alpha(t) + \alpha_0$, where $\alpha(t) = Eu - e$ is a known function and $\alpha_0$ is an unknown constant. With this, equation (21) can be rewritten as:

$$y = \frac{di}{dt} = m\alpha(t) + m\alpha_0 = m\alpha(t) + \beta \tag{26}$$

where $\beta = m\alpha_0$ and $m$ are constants to be estimated. The following asymptotic observer is then proposed:

$$\hat{y} = \hat{m}\alpha(t) + \hat{\beta} \tag{27}$$

$$\frac{d\hat{m}}{dt} = -k\bar{y}\alpha(t) \tag{28}$$

$$\frac{d\hat{\beta}}{dt} = -k\bar{y} \tag{29}$$

where $\bar{y} = \hat{y} - y$, $\bar{\beta} = \hat{\beta} - \beta$, and $\bar{m} = \hat{m} - m$ are the estimation mismatches. The estimation convergence is proven by considering the Lyapunov candidate function:

$$V = \frac{1}{2}\left(\overline{m}^2 + \overline{\beta}^2\right) \tag{30}$$

The time derivative of the Lyapunov function given by equation (30) is calculated to be:

$$\frac{dV}{dt} = -k\overline{y}^2 \leq 0 \tag{31}$$

The estimation process is over when $\overline{y} = \overline{m}\alpha(t) + \overline{\beta} = 0$. Since $\alpha(t)$ is a known time function, $\overline{m}$ and $\overline{\beta}$ has to be tending to zero ($\hat{m}$ and $\hat{\beta}$ are tending to constant values). Thus, values of $m = \hat{m} - \overline{m}$ and $\beta = \hat{\beta} - \overline{\beta}$ are found. To demonstrate the operation of the proposed observer, several computer simulations are presented in Figures 7-8 for the case of sliding mode control of DC-DC buck converter with an asymptotic observer as described by equations (27-29). In these simulations, the reference set point voltage $v_{sp}$ is varied from 2V to 8V and the converter's parameter $m$ is varied in the range $m_{min}$ to $10m_{min}$ where $m_{min} = 1.1765 \times 10^{12} F^{-1} H^{-1}$. As the simulations demonstrate, estimates converge monotonously to the real values during the transient interval of the converter (before reaching $G = 0$).
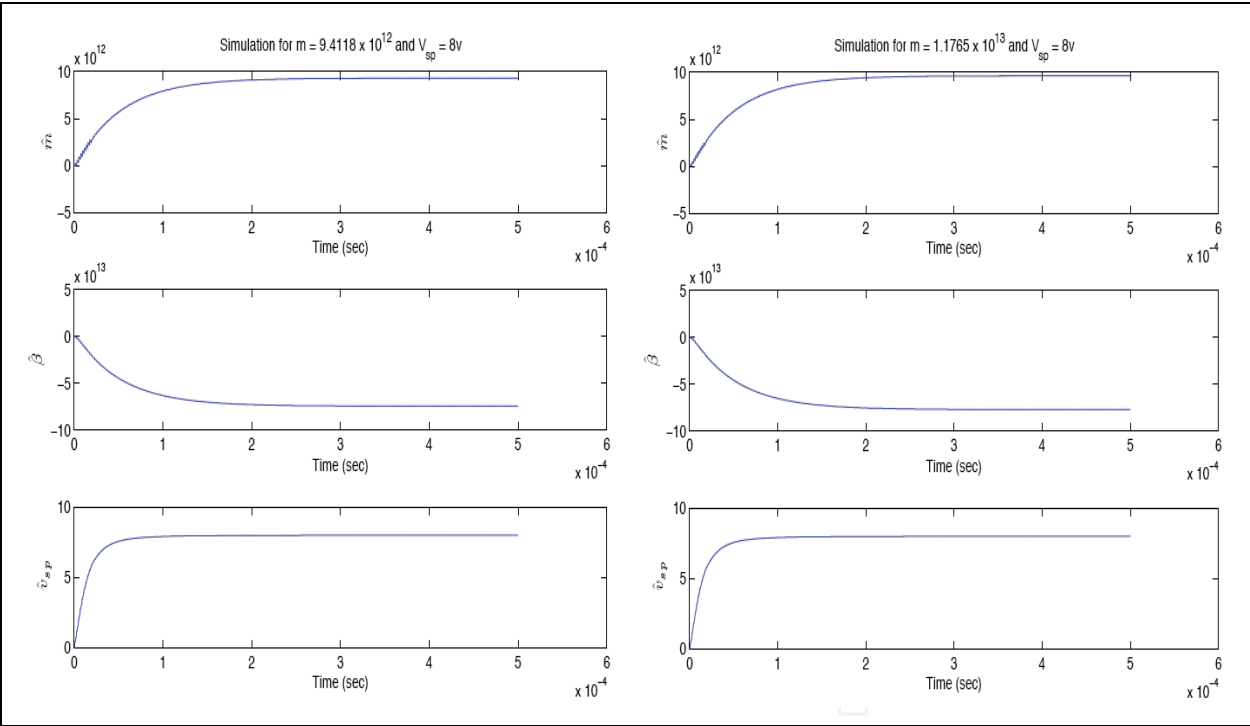


Fig. 7. Sliding Mode PID Control of buck converter with asymptotic observer.

## 5. Modeling and stability analysis of sliding mode controlled single phase DC-DC buck converter

In this section, a different type of DC-DC converter namely the boost converter is discussed. The boost converter is classified as an amplification circuit where the output voltage is a scaled version of the input voltage by a scalar greater than unity. The ideal switch representation of a single-phase boost converter with resistive load is shown in Fig. 9.
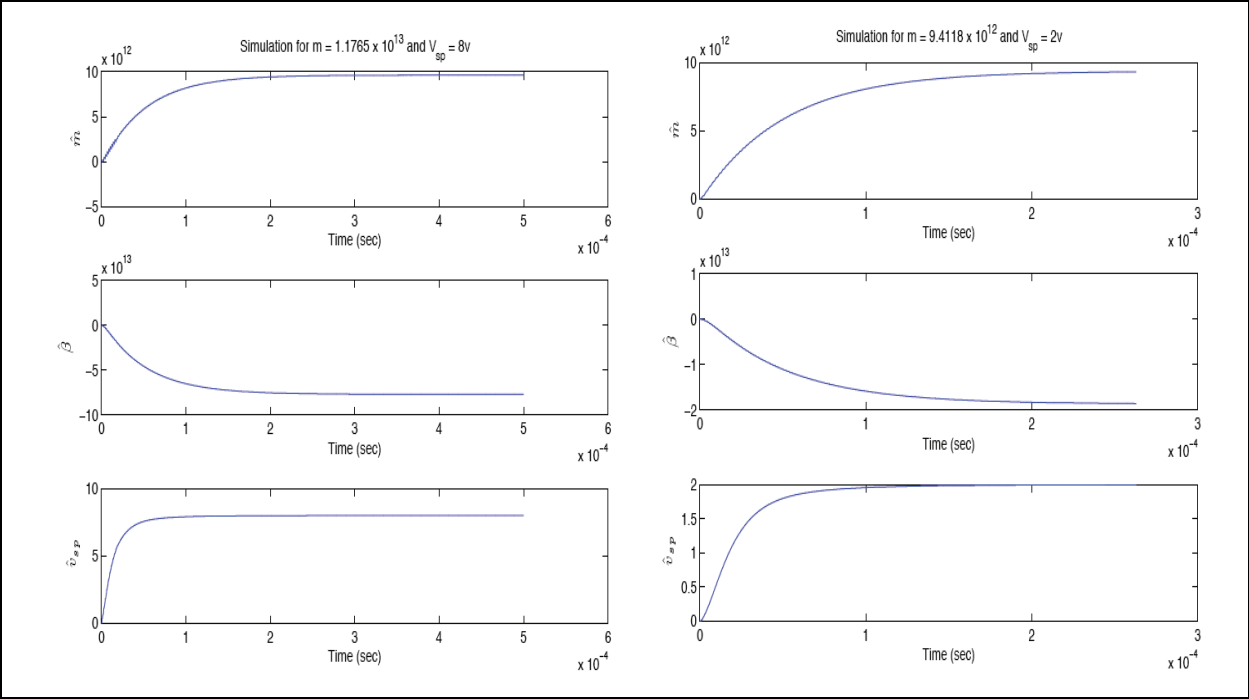
Fig. 8. Sliding Mode PID Control of buck converter with asymptotic observer.

Simple applications of Kirchhoff's current and voltage laws for each resulting circuit topology from the two possible ideal switch's positions allow us to get the system of differential equations governing the dynamics of the boost converter. Thus, we obtain the following *unified* dynamical system model:

$$\frac{dv_C}{dt} = \frac{1}{C}\left[(1-u)i_L - \frac{v_C}{R}\right] \tag{32}$$

$$\frac{di_L}{dt} = \frac{1}{L}\left[E - (1-u)v_C\right] \tag{33}$$

Most often, it is desired to regulate the output voltage $v_C$ to a constant desired value $v_{sp}$ or a to track a given reference signal. Next, we will distinguish between two types of control strategies when dealing with the DC-DC Boost converters. These are the direct and indirect control method. The control objective here is to drive the average of the output voltage $v_C$ to a desired equilibrium value $v_{sp}$.

A. *Direct sliding Mode control of DC-DC Boost converter*

In the direct sliding mode control method, the output voltage $v_C$ is used directly to synthesize a suitable sliding surface yielding the desired objective. For example, consider the following sliding surface and its associated control law:

$$s_{\text{direct}} = v_{sp} - v_C \tag{34}$$

$$u = \frac{1}{2}\left(1 - \text{sign}(s_{\text{direct}})\right) \tag{35}$$

For sliding mode to exist, the condition $s_{\text{direct}}\dot{s}_{\text{direct}} < 0$ must always hold. Thus, we must have $i_L > v_C / R$ since

$$s_{\text{direct}} = 0 \Rightarrow v_C = v_{sp} \tag{36}$$

$$\dot{s}_{\text{direct}} = 0 \Rightarrow \left(1 - u_{eq}\right) i_L = \frac{v_{sp}}{R} \Rightarrow \left(1 - u_{eq}\right) = \frac{v_{sp}}{i_L R} \tag{37}$$

Thus, the motion in sliding mode is governed by the following first order differential equation:

$$\frac{di_L}{dt} = \frac{1}{L}\left( E - \frac{v_{sp}^2}{R i_L} \right) \tag{38}$$

The system has an equilibrium point $i_L^{ss} = v_{sp}^2 / ER$. It is not difficult to see that the system exhibits an unstable equilibrium point (Sira-Ramírez, 2006) and we shall establish this via several approaches.

First, using an approximate linearization approach, the local stability around the equilibrium point of the zero dynamics $i_L^{ss} = v_{sp}^2 / ER$ will be investigated. Expanding the right-hand side of equation (38) into its Taylor series about the point $i_L = i_L^{ss}$, we obtain:

$$\frac{di_L}{dt} = \frac{1}{L}\left( E - \frac{v_{sp}^2}{R i_L} \right)\Bigg|_{i_L = i_L^{ss}} + a_1\left(i_L = i_L^{ss}\right) + \mathrm{O}\left(\bar{i}\right) \tag{39}$$

$$\text{where} \quad a_1 = \frac{d}{di_L}\left( \frac{1}{L}\left( E - \frac{v_{sp}^2}{R i_L} \right) \right)\Bigg|_{i_L = i_L^{ss}} = \frac{E^2 R}{v_{sp}^2}, \quad \bar{i} = i_L - i_L^{ss} \quad \lim_{\bar{i} \to 0} \frac{\mathrm{O}\left(\bar{i}\right)}{\bar{i}} = 0$$

$$\frac{d\bar{i}_L}{dt} = \frac{E^2 R}{v_{sp}^2} \bar{i}_L + H.O.T \tag{40}$$

If we restrict our attention to a sufficiently small neighborhood of the equilibrium point such that the higher order term $\mathrm{O}\left(\bar{i}\right)$ is negligible, then

$$\frac{d\bar{i}_L}{dt} = \frac{E^2 R}{v_{sp}^2} \bar{i}_L \tag{41}$$

Clearly, the equilibrium point $i_L^{ss} = v_{sp}^2 / ER$ is unstable in view of the fact the linearized zero dynamics exhibits a characteristic polynomial with a zero in the right-half part of the complex plane.

Another way of showing instability of the zero dynamics of a direct controlled DC-DC boost converter is to utilize Lyapunov stability theory. For example, consider the following positive definite Lyapunov candidate function:

$$V\left(i_L\right) = \frac{1}{2}\left( E i_L - \frac{v_{sp}^2}{R} \right)^2 \tag{42}$$
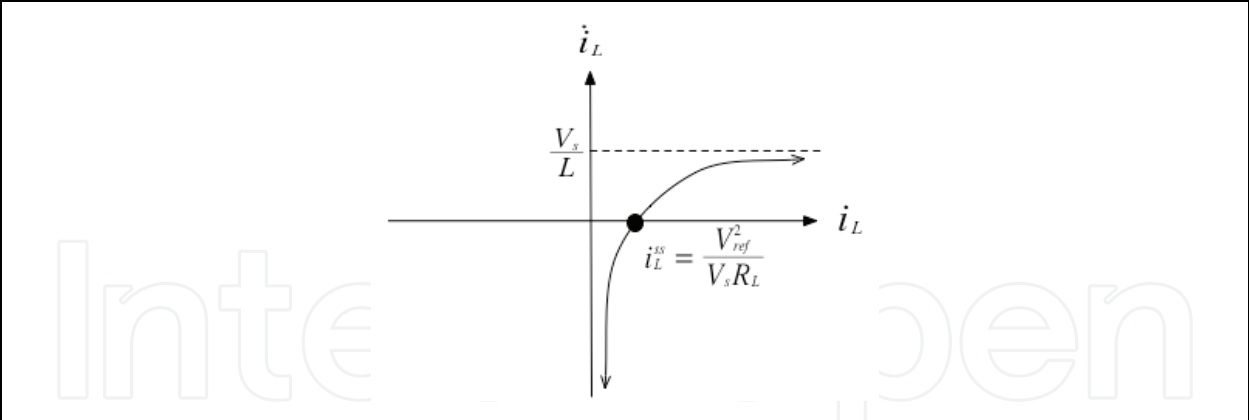
Fig. 9. Phase Portrait diagram for the case of Direct Sliding Mode control of boost converters

The time derivative of the above Lyapunov candidate function (taking into account that $i_L > 0$) is:

$$V(i_L) = \frac{E}{Li_L}\left(Ei_L - \frac{v_{sp}^2}{R}\right)^2 \geq 0 \tag{43}$$

Thus, the system exhibits an unstable zero dynamics. The phase portrait diagram shown in Fig. 9 also confirms this. The fact that the direct voltage controlled boost converters exhibits an unstable equilibrium point is addressed in the control system literature, by stating that the output voltage is a non-minimum phase output. On the contrary, as we will see next, the inductor current is said to be minimum phase output and thus, current controlled boost converter doesn't exhibit an unstable equilibrium point.
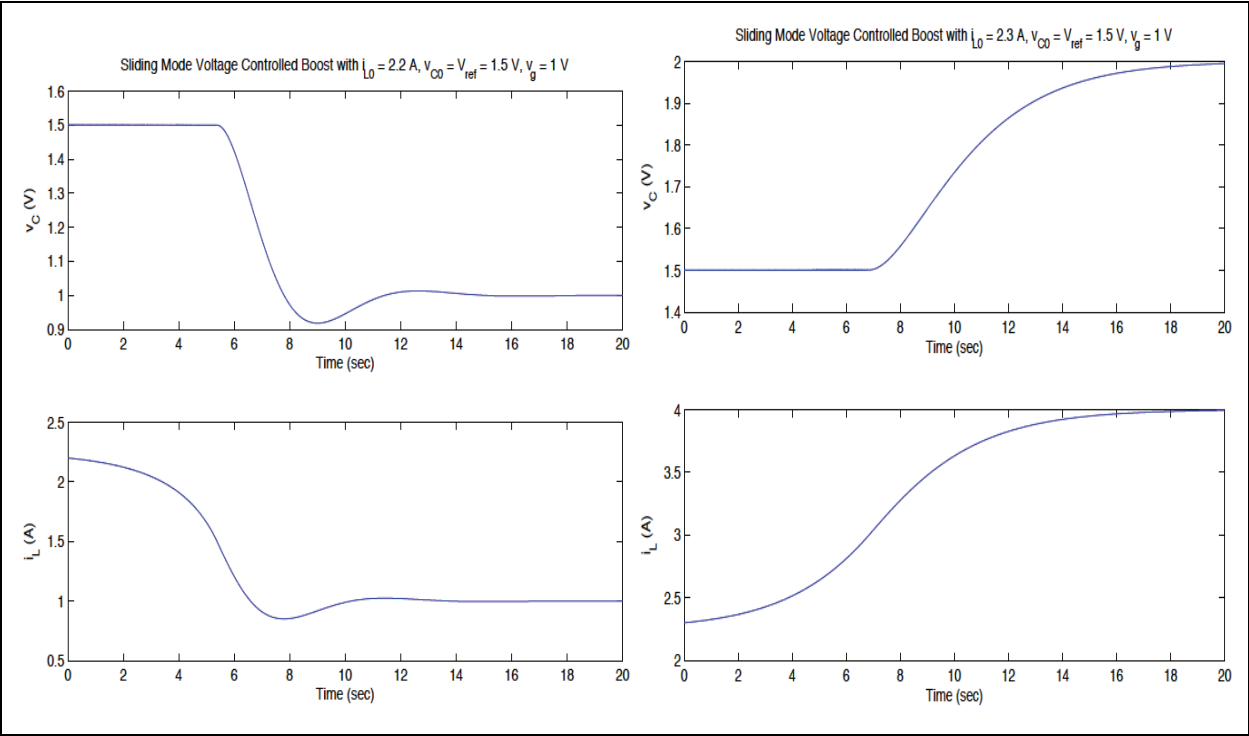


Fig. 10. Sliding Mode Voltage controlled (direct) boost converter

Simulation 1 (left) and 2 (right) in Fig. 10 demonstrates the instability of the zero dynamics for the case of direct voltage controlled DC-DC buck converters. For both of these simulations, the following converter parameters are used: $L = 1H$, $R = 1\Omega$, $C = 1F$, $E = 1V$, $v_{sp} = 1.5V$. Both simulations assume an initial voltage of $v_c(t=0) = 1.5V$. The initial inductor current value is $i_L(t=0) = 2.2A < i_L^{ss} = 2.25A$ for simulation 1 and $i_L(t=0) = 2.3A > i_L^{ss} = 2.25A$ for simulation 2.

B. *Indirect sliding Mode control of DC-DC boost converter*
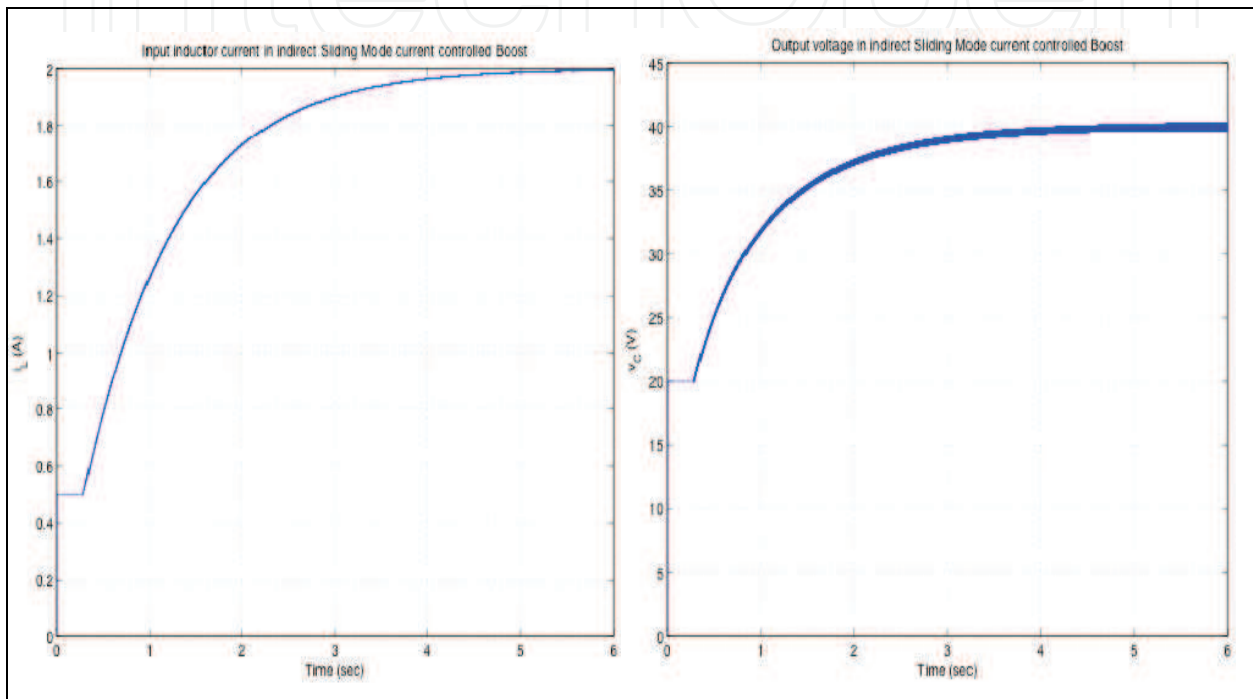


Fig. 11. Sliding Mode current controlled (indirect) boost converter

As demonstrated before, voltage-sliding mode controlled DC-DC boost converters exhibit unstable equilibrium points. The alternative is then to use a sliding surface based on the inductor current such that when it is set to zero, leads to a desired value of the input inductor current in correspondence with the desired output equilibrium voltage. Consider the following indirect current based sliding mode control:

$$s_{\text{indirect}} = i_L - i_{sp} \tag{44}$$

$$u = \frac{1}{2}\left(1 - \text{sign}\left(s_{\text{indirect}}\right)\right) \tag{45}$$

Where $i_{sp}$ is a desired input inductor current calculated in accordance with desired output voltage $v_{sp}$. To calculate the needed $i_{sp}$, we compute the equilibrium point of the system under ideal sliding mode conditions, thus:

$$s_{\text{indirect}} = 0 \Rightarrow i_L = i_{sp}, \quad \dot{s}_{\text{direct}} = 0 \Rightarrow \left(1 - u_{eq}\right) = \frac{E}{v_C}, \quad \frac{dv_C}{dt} = 0 \Rightarrow \left(1 - u_{eq}\right)i_{sp} = \frac{v_C}{R} \Rightarrow i_{sp} = \frac{v_C^2}{ER} \tag{46}$$

For the desire an output voltage $v_{sp}$, the needed set point value for the inductor current is found as

$$i_{sp} = \frac{v_C^2}{ER} \tag{47}$$

The motion after sliding mode is enforced is governed by the following equation:

$$\frac{dv_C}{dt} = \frac{1}{C}\left[\frac{E}{v_C}i_{sp} - \frac{v_C}{R}\right] \tag{48}$$

It is evident that the unique equilibrium point of the zero dynamics is indeed an asymptotically stable one. To proof this, let's consider the following Laypunov candidate function:

$$V = \frac{1}{2}\left(v_C - v_{sp}\right)^2 \tag{49}$$

The time derivative of this Lyapunov candidate function is

$$\begin{aligned}
\dot{V} &= \left(v_C - v_{sp}\right)\frac{1}{C}\left[\frac{E}{v_C}i_{sp} - \frac{v_C}{R}\right] \\
&= \left(v_C - v_{sp}\right)\frac{1}{C}\left[\frac{v_{sp}^2}{v_C R} - \frac{v_C}{R}\right] \\
&= -\frac{1}{Cv_C}\left(v_C - v_{sp}\right)\left(v_C^2 - v_{sp}^2\right) \\
&= -\frac{1}{Cv_C}\left(v_C - v_{sp}\right)^2\left(v_C - v_{sp}\right)
\end{aligned} \tag{50}$$

The time derivative of the Lyapunov candidate function is negative around the equilibrium point $v_{sp}$ given that $v_C > 0$ around the equilibrium. To demonstrate the efficiency of the indirect control method, figure 11 shows simulation result when using the following parameters: $L = 40mH$, $C = 4\mu F$, $R = 40\Omega$, $E = 20V$, $v_{sp} = 40V$.

## 6. Chattering reduction in multiphase DC-DC power converters

One of the most irritating problems encountered when implementing sliding mode control is chattering. Chattering refers to the presence of undesirable finite-amplitude and frequency oscillation when implementing sliding mode controller. These harmful oscillations usually lead to dangerous and disappointing results, e.g. wear of moving mechanical devices, low accuracy, instability, and disappearance of sliding mode. Chattering may be due to the discrete-time implementation of sliding mode control e.g. with digital controller. Another cause of chattering is the presence of unmodeled dynamics that might be excited by the high frequency switching in sliding mode.

Researchers have suggested different methods to overcome the problem of chattering. For example, chattering can be reduced by replacing the discontinuous control action with a continuous function that approximates the $\text{sign}\left(s(t)\right)$ function in a boundary later layer of

the manifold $s(t) = 0$ (Slotine & Sastry, 1983; Slotine, 1984). Another solution (Bondarev, Bondarev, Kostyleva, & Utkin, 1985) is based on the use of an auxiliary observer loop rather than the main control loop to generate chattering-free ideal sliding mode. Others suggested the use of state dependent (Emelyanov, et al., 1970; Lee & Utkin, 2006) or equivalent control dependent (Lee & Utkin, 2006) gain based on the observation that chattering is proportional to the discontinuous control gain (Lee & Utkin, 2006). However, the methods mentioned above are disadvantageous or even not applicable when dealing with power electronics controlled by switches with "ON/OFF" as the only admissible operating states. For example, the boundary solution methods mentioned above replaces the discontinuous control action with a continuous approximation, but control discontinuities are inherent to these power electronics systems and when implementing such solutions techniques such as PWM has to be exploited to adopt the continuous control action. Moreover, commercially available power electronics nowadays can handle switching frequency in the range of hundreds of KHz. Hence, it seems unjustified to bypass the inherent discontinuities in the system by converting the continuous control law to a discontinuous one by means of PWM. Instead, the discontinuous control inputs should be used directly in control, and another method should be investigated to reduce chattering under these operating conditions.

The most straightforward way to reduce chattering in power electronics is to increase the switching frequency. As technology advances, switching devices is now manufactured with enhanced switching frequency (up to 100s KHz) and high power rating. However, power losses impose a new restriction. That is even though switching is possible with high switching frequency; it is limited by the maximum allowable heat losses (resulting from switching). Moreover, implementation of sliding mode in power converters results in frequency variations, which is unacceptable in many applications.

The problem we are dealing with here is better stated as follow. We would like first to control the switching frequency such that it is set to the maximum allowable value (specified by the heat loss requirement) resulting in the minimum possible chattering level. Chattering is then reduced under this fixed operating switching frequency. This is accomplished through the use of interleaving switching in multiphase power converters where harmonics at the output are cancelled (Lee, 2007; Lee, Uktin, & Malinin, 2009). In fact, several attempts to apply this idea can be found in the literature. For example, phase shift can be obtained using a transformer with primary and secondary windings in different phases. Others tried to use delays, filters, or set of triangular inputs with selected delays to provide the desired phase shift (Miwa, Wen, & Schecht, 1992; Xu, Wei, & Lee, 2003; Wu, Lee, & Schuellein, 2006). This section presents a method based on the nature of sliding mode where phase shift is provided without any additional dynamic elements. The section will first presents the theory behind this method. Then, the outlined method will be applied to reduce chattering in multiphase DC-DC buck and boost converters.

A. *Problem statement: Switching frequency control and chattering reduction in sliding mode power converters*

Consider the following system with scalar control :

$$\dot{x} = f(x,t) + b(x,t)u \quad x, f, b \in \mathbb{R}^n \tag{51}$$

Here, control is assumed to be designed as a continuous function of the state variables, i.e. $u_0(x)$. In electric motors with current as a control input, it is common to utilize the so-called "cascaded control". Power converters usually use PWM as principle operation mode to

implement the desired control. One of the tools to implement this mode of operation is sliding mode control. A block diagram of possible sliding mode feedback control to implement PWM is shown in fig. 12. When sliding mode is enforced along the switching line $s = u_0(x) - u$, the output $u$ tracks the desired reference control input $u_0(x)$. Sliding mode existence condition can be found as follow:

$$s = u_0(x) - u, \quad \dot{u} = v = M \operatorname{sign}(s), \quad M > 0$$

$$\Rightarrow \dot{s} = g(x) - M \operatorname{sign}(s), \quad g(x) = \operatorname{grad}^{\mathrm{T}}(u_0)(f + bu)$$

(52)

Thus, for sliding mode to exist, we need to have $M > |g(x)|$.
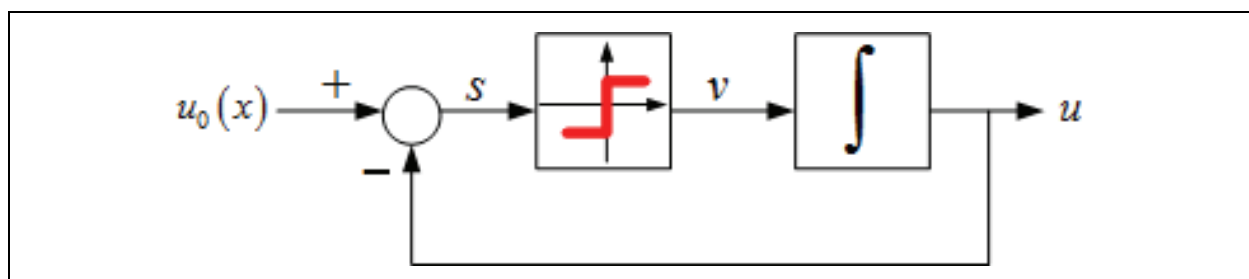


Fig. 12. Sliding mode control for simple power converter model
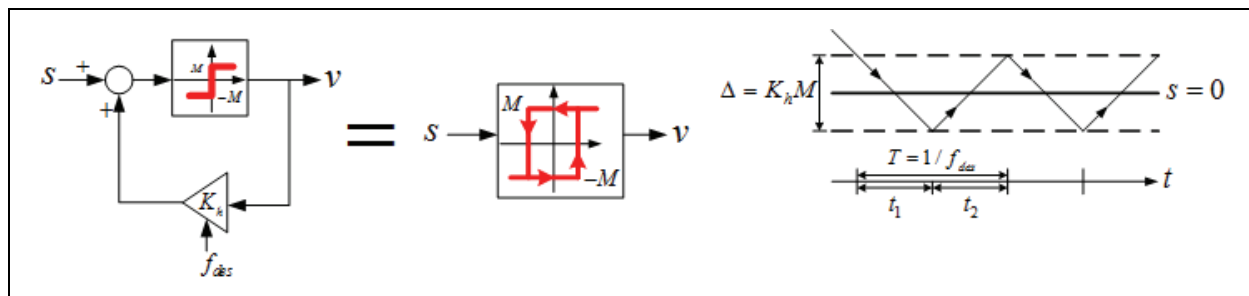


Fig. 13. Implementation of hysteresis loop with width $\Delta = K_h M$. Oscillations in the vicinity of the switching surface is shown in the right side of the figure. Frequency control is performed by changing the width of a hysteresis loop in switching devices (Nguyen & Lee, 1995; Cortes & Alvarez, 2002)

To maintain the switching frequency at a desired level $f_{des}$, control is implemented with a hysteresis loop (switching element with positive feedback as shown in fig. 13). Assuming that the switching frequency is high enough such that the state $x$ can be considered constant within time intervals $t_1$ and $t_2$ in fig. 13, the switching frequency can be calculated as:

$$f = \frac{1}{t_1 + t_2}, \quad t_1 = \frac{\Delta}{M - g(x)}, \quad t_2 = \frac{\Delta}{M + g(x)}$$

(53)

Thus, the width of the hysteresis loop needed to result in a switching frequency $f_{des}$ is:

$$\Delta = \frac{1}{f_{des}} \frac{M^2 - g^2(x)}{2M}$$

(54)

$f_{des}$ is usually specified to be the maximum allowable switching frequency resulting in the minimum possible level of chattering. However, this chattering level may still not be acceptable. Thus, the next step in the design process is to reduce chattering under this operating switching frequency by means of harmonics cancellation, which will be discussed next.
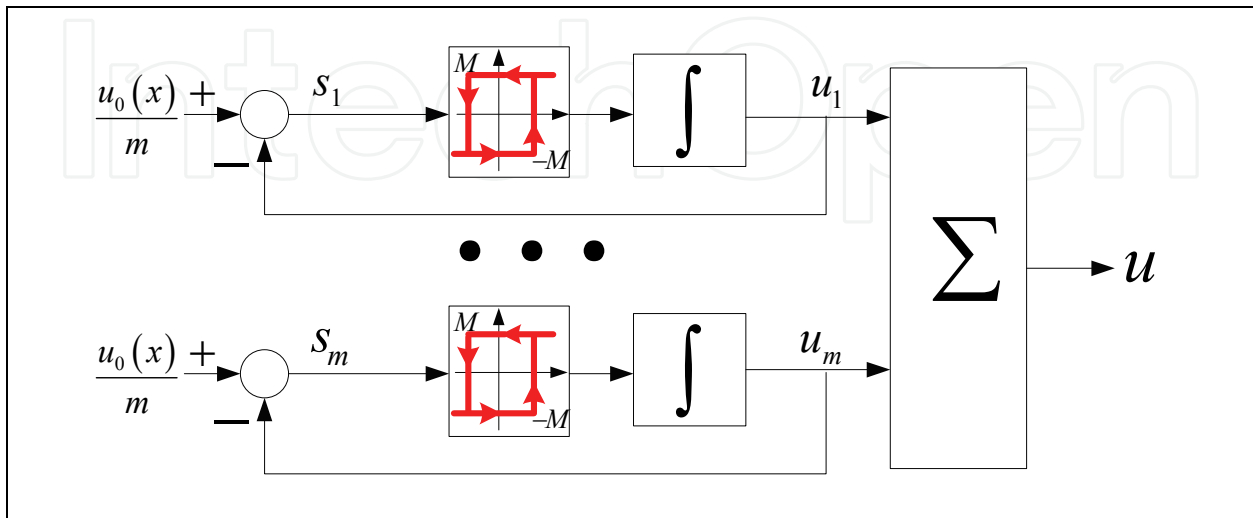


Fig. 14. m-phase power converter with evenly distributed reference input

Let's assume that the desired control $u_0(x)$ is implemented using $m$ power converters, called "multiphase converter" (Fig. 14) with $s_i = u_0/m - u_i$ where $i = 1, 2, \text{K}, m$. The reference input in each power converter is $u_0/m$. If each power converters operates correctly, the output $u$ will track the desired control $u_0(x)$. The amplitude $A$ and frequency $f$ of chattering in each power converter are given by:

$$A = \frac{\Delta}{2}, \; f = \frac{M^2 - (g(x)/m)^2}{2M\Delta} \tag{55}$$

The amplitude of chattering in the output $u$ depends on the amplitude and phase of chattering in each leg and, in the worst-case scenario, can be as high as $m$ times that in each individual phase. For the system in Fig. 14, phases depend on initial condition and can't be controlled since phases in each channel are independent in this case. However, phases can be controlled if channels are interconnected (thus not independent) as we will be shown later in this section.

Now, we will demonstrate that by controlling the phases between channels (through proper interconnection), we can cancel harmonics at the output and thus reduce chattering. For now, let's assume that $m$ – phases power converter is designed such that the frequency of chattering in each channel is controlled such that it is the same in each phase $(f = 1/T)$. Furthermore, the phase shift between any two subsequent channels is assumed to be $T/m$. Since chattering is a periodic channel, it can be represented by its Fourier series with frequencies $\omega_k = k\omega$ where $\omega = 2\pi/T$ and $k = 1, 2, \text{K}, \infty$. The phase difference between the first channel and $i$th channel is given by $\phi_i = 2\pi/(\omega m)$. The effect of the $k$th harmonic in the output signal is the sum of the individual $k$th harmonics from all channels and can be calculated as:

$$\sum_{i=0}^{m-1} \sin\left(\omega_k\left(t - \frac{2\pi}{\omega m}i\right)\right) = \sum_{i=0}^{m-1} \text{Im}\left[\exp\left(j\omega_k\left(t - \frac{2\pi}{\omega m}i\right)\right)\right] \tag{56}$$
$$= \text{Im}\left(Z\exp(j\omega_k t)\right)$$
$$\text{where} \quad Z = \sum_{i=0}^{m-1} \exp\left(-j\frac{2\pi k}{m}i\right)$$

Now consider the following equation:

$$Z\exp\left(-j\frac{2\pi k}{m}\right) = \sum_{i=0}^{m-1}\exp\left(-j\frac{2\pi k}{m}(i+1)\right) = \sum_{i'=1}^{m}\exp\left(-j\frac{2\pi k}{m}i\right) = Z \tag{57}$$

The solution to equation (57) is that either $\exp(-j2\pi k / m) = 1$ or $Z = 0$. Since we have $\exp(-j2\pi k / m) = 1$ when $k / m$ is integer, i.e. $k = m, 2m, \mathsf{K}$, then we must have $Z = 0$ for all other cases. This analysis means that all harmonics except for $lm$ with $l = 1, 2, \mathsf{K}$ are suppressed in the output signal. Thus, chattering level can be reduced by increasing the number of phases (thus canceling more harmonics at the output) provided that a proper phases shift exists between any subsequent phases or channels.
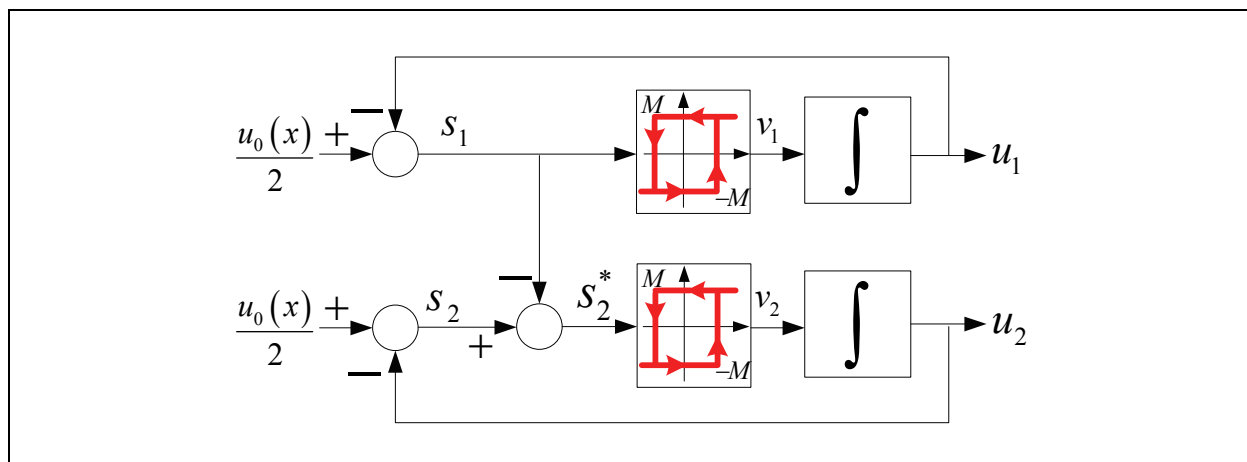


Fig. 15. Interconnection of channels in two-phase power converters to provide desired phase shift

The next step in design process is to provide a method of interconnecting the channels such that a desired phase shift is established between any subsequent channels. To do this, consider the interconnection of channels in the two-phase power converter model shown in Fig 15. The governing equations of this model are:

$$s_1 = u_0 / 2 - u_1, \quad s_2 = u_0 / 2 - u_2, \quad s_2^* = s_2 - s_1 \tag{58}$$

The time derivative of $s_1$ and $s_2^*$ is are given by:

$$\dot{s}_1 = a - M\,\text{sign}(s_1), \quad a = g(x) / m, m = 2, \quad g(x) = \text{grad}^T(u_0)(f + bu) \tag{59}$$

$$\dot{s}_2^* = M\,\text{sign}(s_1) - M\,\text{sign}(s_2^*) \tag{60}$$

Consider now the system behavior in the $s_1, s_2^*$ plane as shown in Fig. 16 and 17. In Fig. 16, the width of hysteresis loops for the two sliding surfaces $s_1 = 0$ and $s_2^* = 0$ are both set to $\Delta$. As can be seen from figure 16, the phase shift between the two switching commands $v_1$ and $v_2$ is always $T / 4$ for any value of $\Delta$, where $T$ is the period of chattering oscillations $T = 2\Delta / m$. Also, starting from any initial conditions different from point 0 (for instance $0'$ in Fig. 16), the motion represented in Fig. 16 will appear in time less than $T / 2$.
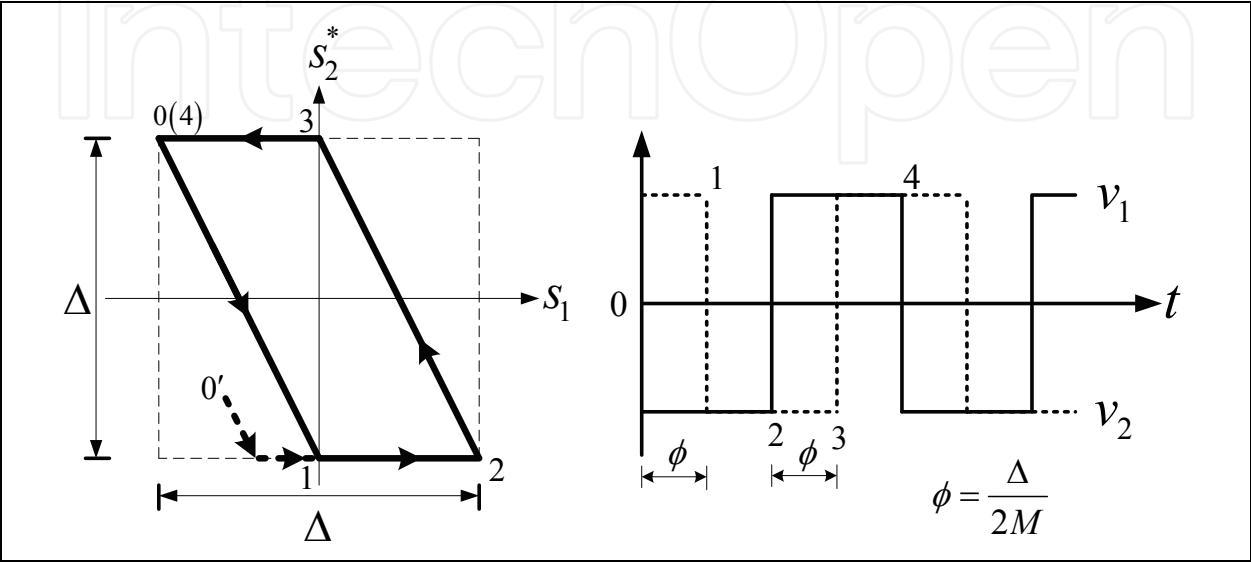


Fig. 16. System behavior in $s$ plane with $\alpha = 1$ and $a > 0$
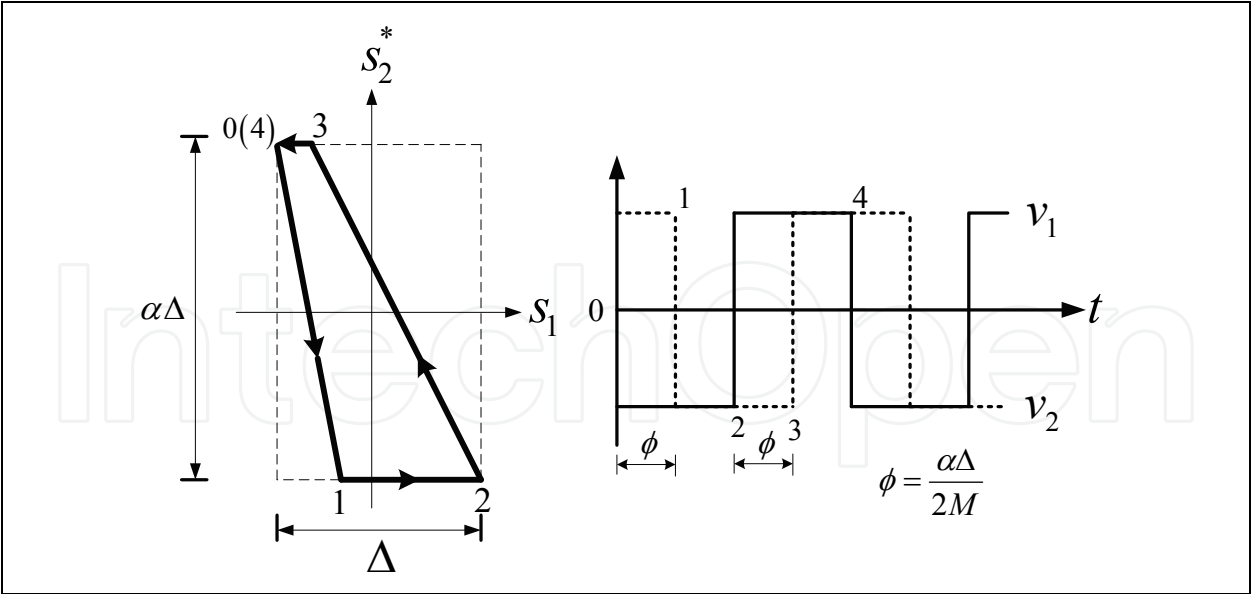


Fig. 17. System behavior in $s$ plane with $\alpha > 1$ and $a > 0$

If the width of the hysteresis loop for the two sliding surface $s_1 = 0$ and $s_2^* = 0$ are set to $\Delta$ and $\alpha\Delta$ respectively (as in Fig. 17), the phase shift between the two switching commands $v_1$ and $v_2$ can be controlled by proper choice of $\alpha$. The switching frequency $f$ and phase shift $\phi$ are given by:

$$T = \frac{1}{f} = \frac{\Delta}{M-a} + \frac{\Delta}{M+a} = \frac{2M\Delta}{M^2 - a^2}, \tag{61}$$

$$\phi = \frac{\alpha\Delta}{2M}, \quad a = \frac{g(x)}{m}, \quad g(x) = g(x) = \mathrm{grad}^T(u_0)(f + bu) \tag{62}$$

To preserve the switching cycle, the following condition must always be satisfied:

$$\frac{\alpha\Delta}{2M} \le \frac{\Delta}{M + |a|} \tag{63}$$

Thus, to provide a phase shift $\phi = T / m$, where $m$ is the number of phases, we choose the parameter $\alpha$ as:

$$\alpha = \frac{4M^2}{m\left(M^2 - a^2\right)} \tag{64}$$

The function $a$ is assumed to be bounded i.e. $|a| < a_{max} < M$. With this, condition (63) can be rewritten as:

$$m > \frac{2\Delta}{M - a_{max}} \quad \text{or} \quad |a| \le M\left(1 - \frac{2}{m}\right) m \ge 2 \tag{65}$$

It is important to make sure that the selected $\alpha$ doesn't lead to any violation of condition (63) or (65) which might lead to the destruction of the switching cycle. Thus, equation (63) is modified to reflect this restriction, i.e.

$$\alpha = \begin{cases} \dfrac{4M^2}{m\left(M^2 - a^2\right)} & \text{if} \quad |a| < M\left(1 - \dfrac{2}{m}\right) \\[4mm] \dfrac{2M}{M + |a|} & \text{if} \quad M\left(1 - \dfrac{2}{m}\right) \le |a| < M \end{cases} \tag{66}$$
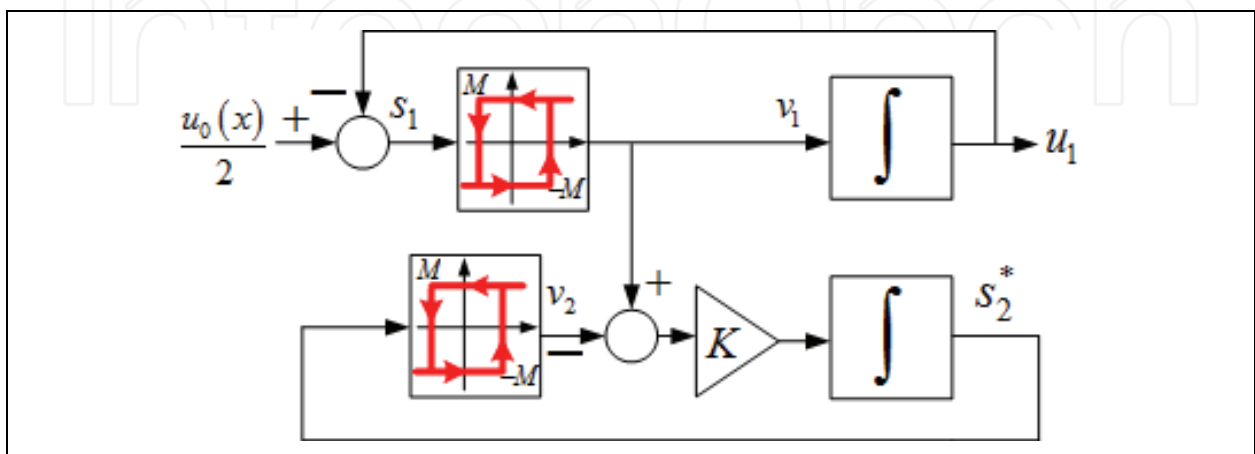


Fig. 18. Master-slave two-phase power converter model

Another approach in which a frequency control is applied for the first phase and open loop control is applied for all other phases is shown in Fig. 18. In this approach (called master-slave), the first channel (master) is connected to the next channel or phase (slave) through an additional first order system acting as a phase shifter. This additional phase shifter system acts such that the discontinuous control $v_2$ for the slave has a desired phase shift with respect to the discontinuous control $v_1$ for the master without changing the switching frequency. In this system, we have:

$$s_1 = \frac{1}{m} u_0 - u_1, \quad m = 2 \tag{67}$$

$$\dot{s}_1 = a - M\text{sign}(s_1), \quad a = \frac{g(x)}{m}, \quad g(x) = \text{grad}^T u_0 (f + bu) \tag{68}$$

$$\dot{s}_2^* = KM \left( \text{sign}\left(s_1\right) - \text{sign}\left(s_2^*\right)\right), \tag{69}$$

The phase shift between $v_1$ and $v_2$ (based on s-plane analysis) is given by

$$\phi = \frac{\Delta}{2KM} \tag{70}$$

Thus, the value of gain $K$ needed to provide a phase shift of $T / m$ is:

$$K = \frac{m\left(M^2 - a^2\right)}{4M^2} \tag{71}$$

Please note that, $K = 1 / \alpha$ should be selected in compliances with equation (63) to preserve the switching cycle as discussed previously. To summarize, a typical procedures in designing multiphase power converters with harmonics cancellation based chattering reduction are:

1. Select the width of the hysteresis loop (or its corresponding feedback gain $K_h$ ) to maintain the switching frequency in the first phase at a desired level (usually chosen to be the maximum allowable value corresponding to the maximum heat power loss tolerated inn the system).
2. Determine the number of needed phases for a given range of function $a$ variation.
3. Find the parameter $\alpha$ such that the phase shift between any two subsequent phases or channels is equal to $1 / m$ of the oscillation period of the first phase.

Next, we shall apply the outlined procedures to reduce chattering in sliding mode controlled multiphase DC-DC buck and boost converters.

## 7. Chattering reduction in multiphase DC-DC buck converters

Consider the multiphase DC-DC buck converter depicted in Fig. 19. The shown converter composed of $n = 4$ legs or channels that are at one end controlled by switches with switching commands $u_i \in \{0,1\}, i = 1, \mathsf{K}, n$, and all connected to a load at the other end. A $n$ – dimensional control law $u = [u_1, u_2, \ldots, u_n]^T$ is to be designed such that the output voltage across the resistive load/capacitance converges to a desired unknown reference

voltage $v_{sp}$ under the following assumptions (similar to the single-phase buck converter discussed earlier in this chapter):

- Values of inductance $L$ and capacitance $C$ are unknown, but their product $m = 1/LC$ is known.
- Load resistance $R$ and input resistance $r$ are unknown.
- Input voltage $E$ is assumed to be constant floating in the range $[E_{\min}, E_{\max}]$.
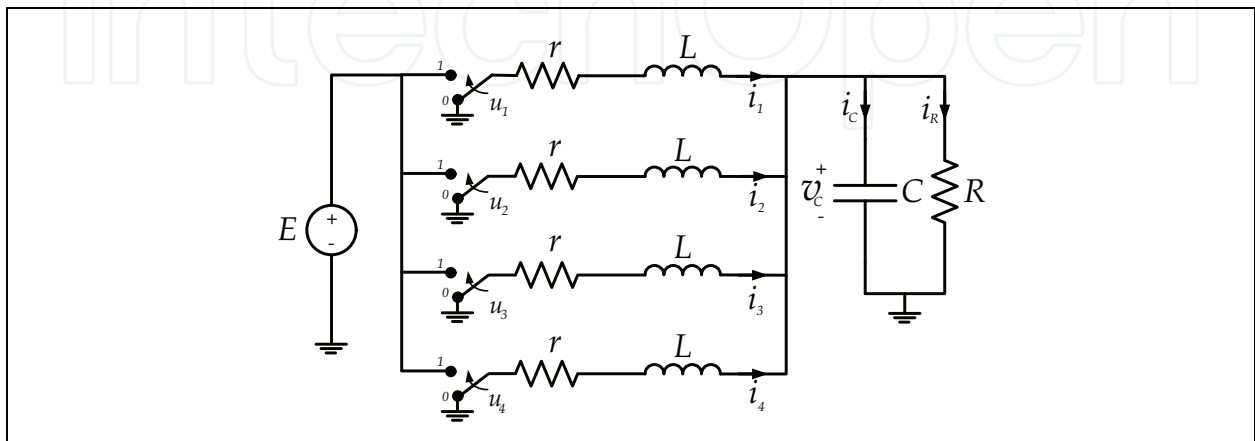- The only measurement available is that of the voltage error $e = v_C - v_{sp}$.



Fig. 19. 4-phase DC-DC buck converter

The dynamics of $n-$ phase DC-DC buck converter are governed by the following set of differential equations:

$$\dot{i}_k = \frac{1}{L}\left(Eu_k - ri_k - v_C\right), \quad k = 1,\dots,n \tag{72}$$

$$\dot{v}_c = \frac{1}{C}\left(\sum_{k=1}^{n} i_k - i_R\right) \tag{73}$$

A straightforward way to approach this problem is to design a PID sliding mode controlled as done before for the single-phase buck converter cases discussed earlier in this chapter. To reduce chattering, however, we exploit the additional degree of freedom offered by the multiphase buck converter in cancelling harmonics (thus reduce chattering) at the output. Based on the design procedures outlined in the previous section, the following controller is proposed:

$$\tilde{v} = L_1\left(v_C - v_{sp}\right) \tag{74}$$

$$\tilde{\dot{i}} = m\left[u_1 - \tilde{v} + L_2\left(v_C - v_{sp}\right)\right], \quad \text{m=1/LC} \tag{75}$$

$$s_1 = \frac{1}{c\sqrt{m}}\left(v_C - v_{sp}\right) + \frac{1}{m}\tilde{i} \tag{76}$$

$$\dot{s}_k = Kb\left[\text{sign}(s_{k-1}) - \text{sign}(s_k)\right], \quad k = 2,\dots,n, \quad b = \frac{1}{2} \tag{77}$$

$$u_k = \frac{1}{2}\left(1 - \text{sign}(s_k)\right), \quad k = 1,...,n \tag{78}$$

The time derivative of the sliding surface in the first phase is given by:

$$\dot{s}_1 = a - b\,\text{sign}(s_1) \quad a = \frac{1}{c\sqrt{m}C}\left(\sum_{k=1}^{n} i_k - i_R\right) + \frac{1}{2} + L_2\left(v_C - v_{sp}\right) - \tilde{v}, \quad b = \frac{1}{2} \tag{79}$$

To preserve the switching cycle, the gain $K = 1/\alpha$ is to be selected in accordance with equation (66). Thus, we must have

$$K = \begin{cases} \dfrac{n}{4}\left(1 - \left(\dfrac{a}{b}\right)^2\right) & \text{if } \left|\dfrac{a}{b}\right| < \left(1 - \dfrac{2}{n}\right) \\[3mm] \dfrac{1}{2}\left(1 + \left|\dfrac{a}{b}\right|\right) & \text{if } \left(1 - \dfrac{2}{n}\right) \leq \left|\dfrac{a}{b}\right| < 1 \end{cases} \tag{80}$$

As we can see from equation (80), the parameter $a/b$ is needed to implement the controller. However, this parameter can be easily obtained by passing the signal $\text{sign}(s_1)$ as the input to a low pass filter. The output of the low pass filter is then a good estimate of the needed parameter. This is because when sliding mode is enforced along the switching surface $S_1 = 0$, we also have $\dot{s}_1 = 0$ leading to the conclusion that $\left(\text{sign}(s_1)\right)_{eq} = a/b$. Of course, controller parameters $c$, $L_1$, and $L_2$ must be chosen to provide stability for the error dynamics similar to the single-phase case discussed earlier in this chapter. Using the above-proposed controller, the switching frequency is first controlled in the first phase. Then, a phase shift of $T/n$ (where $T$ is chattering period, and $n$ is the number of phases) between any subsequent channels is provided by proper choice of gain $K$ resulting in harmonics cancellation (and thus chattering reduction) at the output. Fig. 20 shows simulation result for a 4-phase DC-DC buck converter with sliding mode controller as in equations (74-78). The parameters used in this simulation are $L = 0.1\mu H$, $C = 8.5\mu F$, $R = 0.01\Omega$, $E = 12V$, $c = 9.2195 \times 10^{-4}$, $L_1 = -10^4$, and $L_2 = 199.92$. The reference voltage $v_{sp}$ is set to be $2.9814V$. As evident from the simulation result, the switching frequency is maintained at $f = 1/T = 100\text{KHz}$. Also, a desired phase shift of $T/4$ between any subsequent channels is provided leading to harmonics cancellation (and thus chattering reduction) at the output.

## 8. Chattering reduction in multiphase DC-DC boost converters

In this section, chattering reduction by means of harmonics cancellation in multiphase DC-DC boost converter is discussed (Al-Hosani & Utkin, 2009). Consider the multiphase ($n = 4$) DC-DC boost converter shown in Fig. 21. The shown converter is modeled by the following set of differential equations:

$$\dot{i}_k = \frac{1}{L}\left(E - (1 - u_k)v_C\right) \tag{81}$$

$$\dot{v}_C = \frac{1}{C}\left(\sum_{k=1}^{n}(1 - u_K)i_k - \frac{1}{R}v_C\right) \tag{82}$$
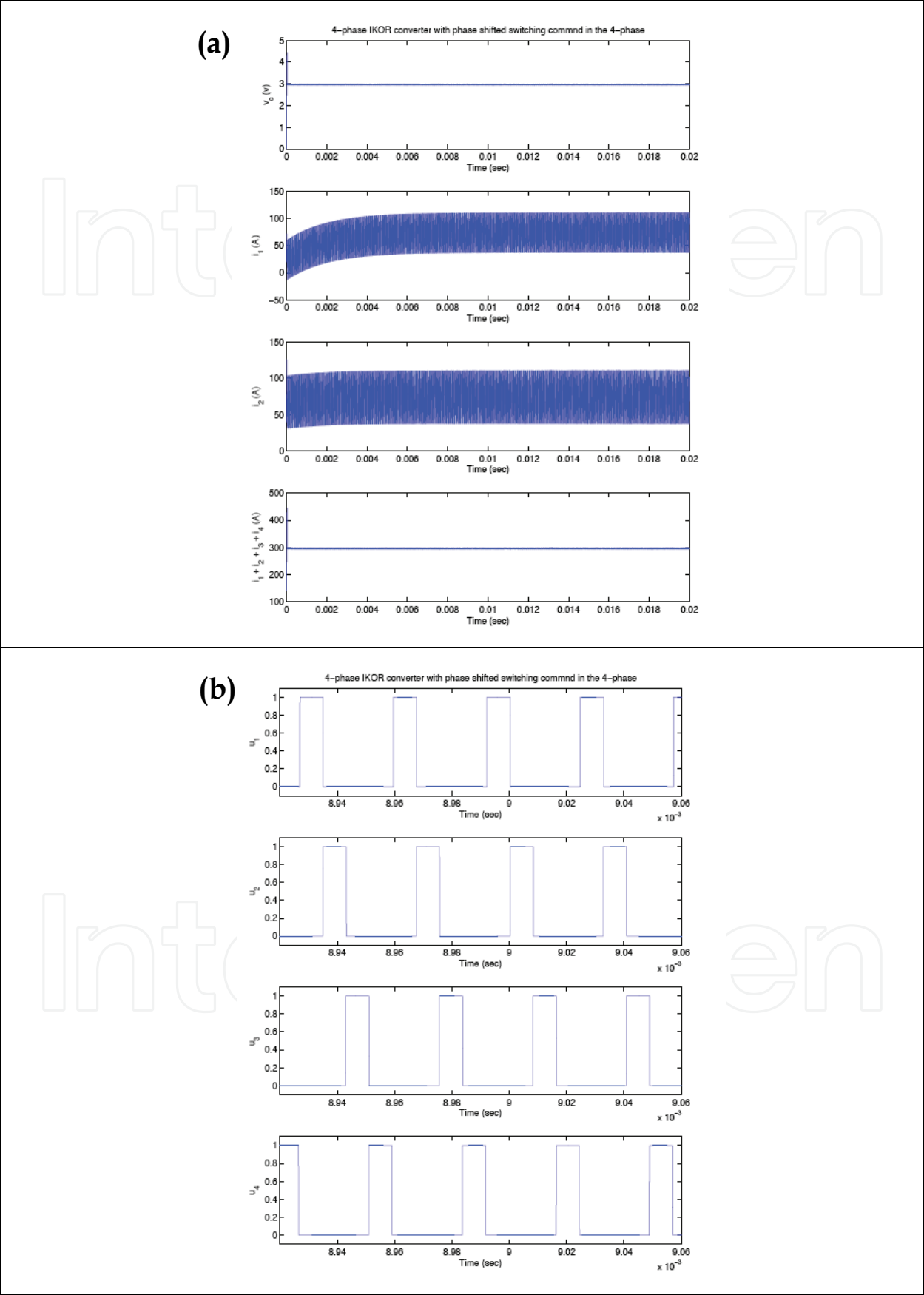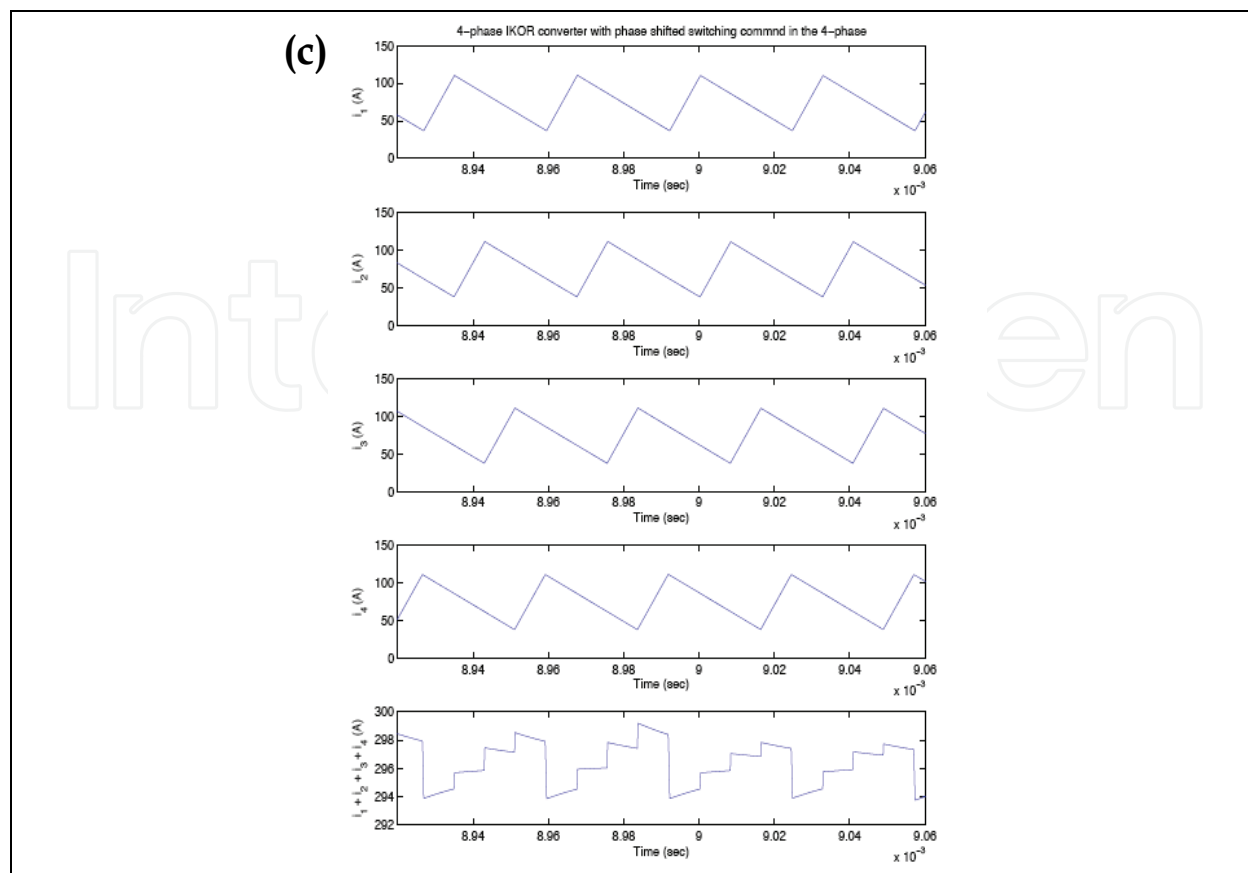
Fig. 20. Simulation of sliding mode controlled 4-phase DC-DC buck converter: (a): the top figure shows the output voltage across the resistive load/capacitor. Shown also are currents in the 1st and 2nd phases as well as current flowing through the load. (b): Switching Frequency is controlled in the first phase and a phase shift of a quarter period is provided between any two subsequent channels. (c): Zoomed in picture of the 4 currents as well as the output current going through the load. The amount of chattering is reduced at the output through harmonics cancellation provided by the phase-shifted currents.

where $v_C$ is the voltage across the resistive load/capacitor, $i_k$, $k = 1, \ldots, n$ is the current flowing through $k^{th}$ leg, and $E$ is the input voltage. A $n$-dimensional control law $u = [u_1, u_2, \ldots, u_n]^T$ is to be designed such that the output voltage $v_C$ across the capacitor/resistive load converges to a desired known constant reference value $v_{sp}$. It is assumed that all currents $i_k$, $k = 1, \ldots, n$ and the output voltage $v_C$ are measured. Also, the inductance $L$ and capacitance $C$ are assumed to be known.

The ultimate control's goal is to achieve a constant output voltage of $v_{sp}$. As discussed earlier in this chapter, direct control of the output voltage for boost converters results in a non-minimum phase system and therefore unstable controller. Instead, we control the output voltage indirectly by controlling the current flowing through the load to converge to a steady state value $i_0$ that results in a desired output voltage $v_{sp}$. By analyzing the steady-state behavior of the multiphase boost converter circuit, the steady state value of the sum of all individual currents in each phase is given by:

$$\sum_{k=1}^{n} i_k^{ss} = \frac{v_{sp}^2}{RE} = i_0 \tag{83}$$
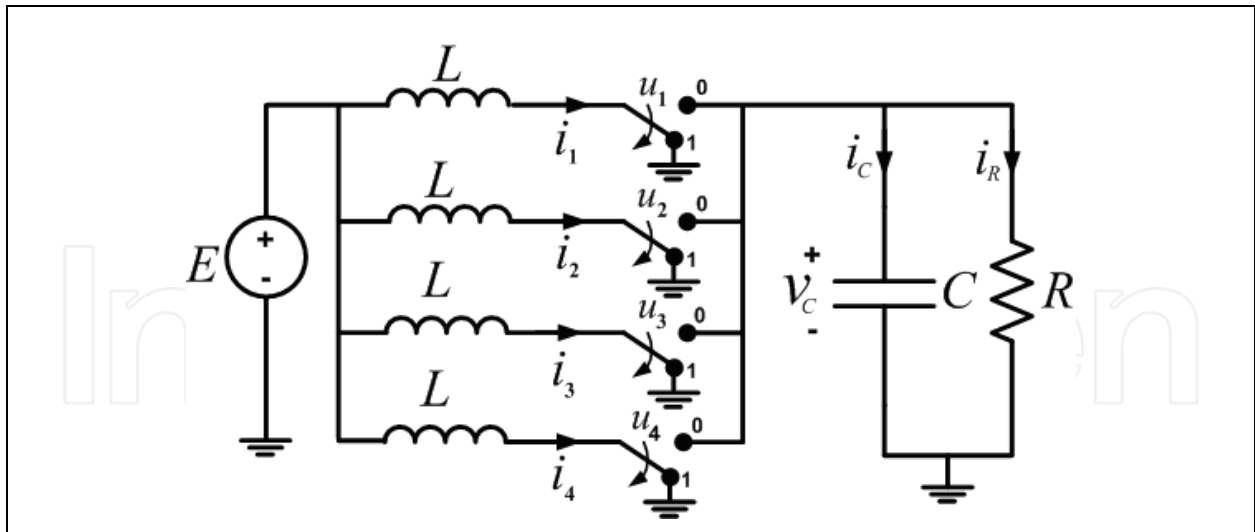
Fig. 21. 4-phase DC-DC boost converter

A sliding mode controller is designed such that each leg of the total $n$ phases supplies an equal amount $i_0 / n$ at steady state resulting in a total current of $i_0$ flowing through the resistive load at the output. To reduce chattering (through harmonics cancellation), the switching frequency $f = 1/T$ is first controlled in the 1st phase. Then a phase shift of $T/n$ is provided between any two subsequent phases. Assuming that the switching device is implemented with a hysteresis loop of width $\Delta$ for the first phase, and $\alpha\Delta$ for all other phases, we propose a controller with the following governing equations:

$$s_k = i_k - i_0 / n, \quad k = 1, \ldots, n \tag{84}$$

$$s_2^* = s_2 - s_1 \tag{85}$$

$$s_k^* = s_k - s_{k-1}^*, \quad k = 3, \ldots, n \tag{86}$$

The switching commands for each leg in the multiphase boost converter are given by:

$$u_1 = \frac{1}{2}\left(1 - \operatorname{sign}(s_1)\right) \tag{87}$$

$$u_k = \frac{1}{2}\left(1 - \operatorname{sign}(s_k^*)\right), \quad k = 2, \ldots, n \tag{88}$$

The time derivative of the switching surfaces are given by:

$$\dot{s}_1 = a - b \operatorname{sign}(s_1), \quad a = E/L - v_C/2L, \quad b = v_C/2L \tag{89}$$

$$\dot{s}_2^* = b \operatorname{sign}(s_1) - b \operatorname{sign}(s_2^*) \tag{90}$$

$$\dot{s}_k^* = b \operatorname{sign}(s_{k-1}^*) - b \operatorname{sign}(s_k^*), \quad k = 3, \ldots, n \tag{91}$$
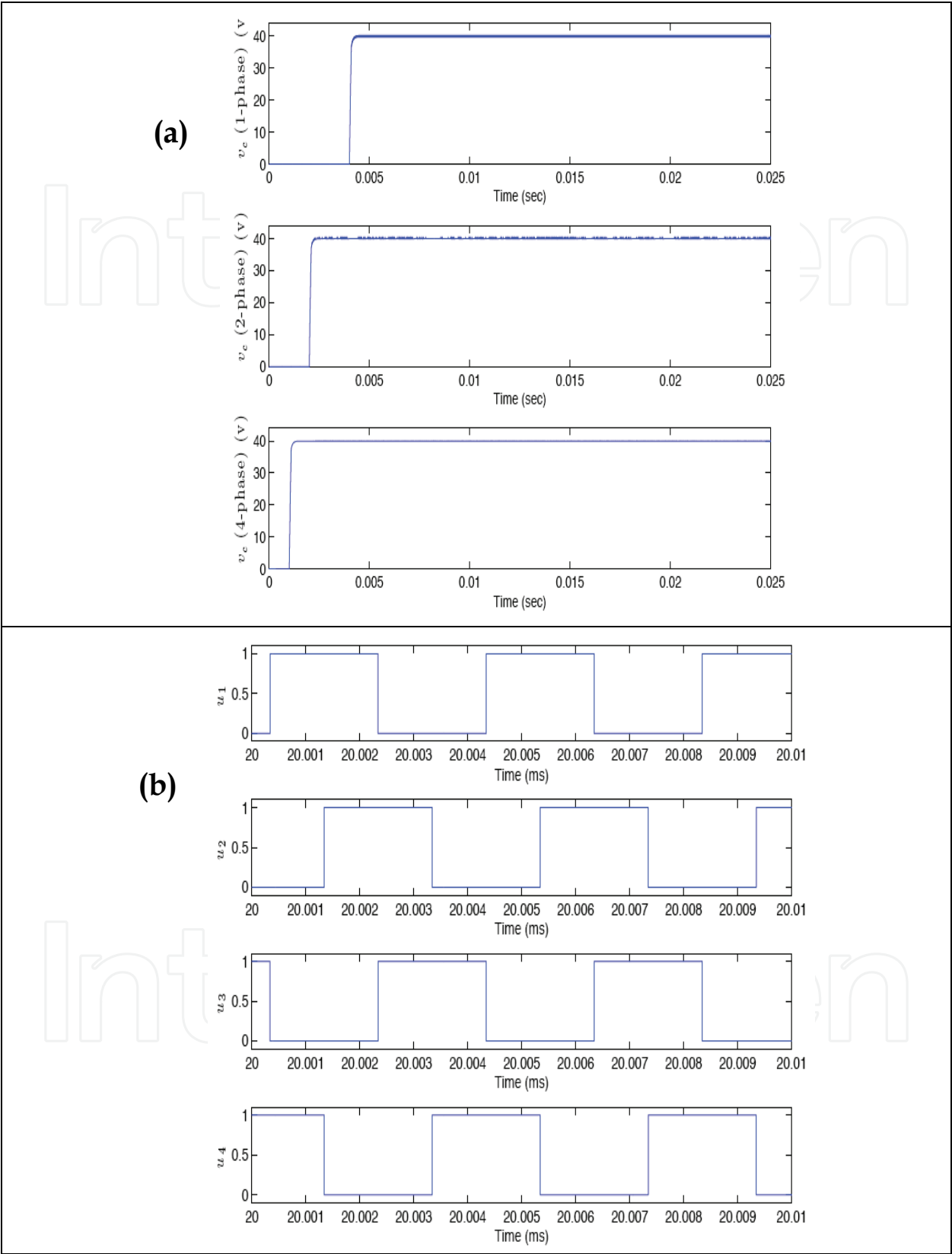
Fig. 22. Simulation of 1-phase, 2-phases and 4-phases Boost converter with $v_{sp} = 40\text{V}$ .
Figure (b) shows the switching command for the case of 4-phase boost converter. Clearly, a
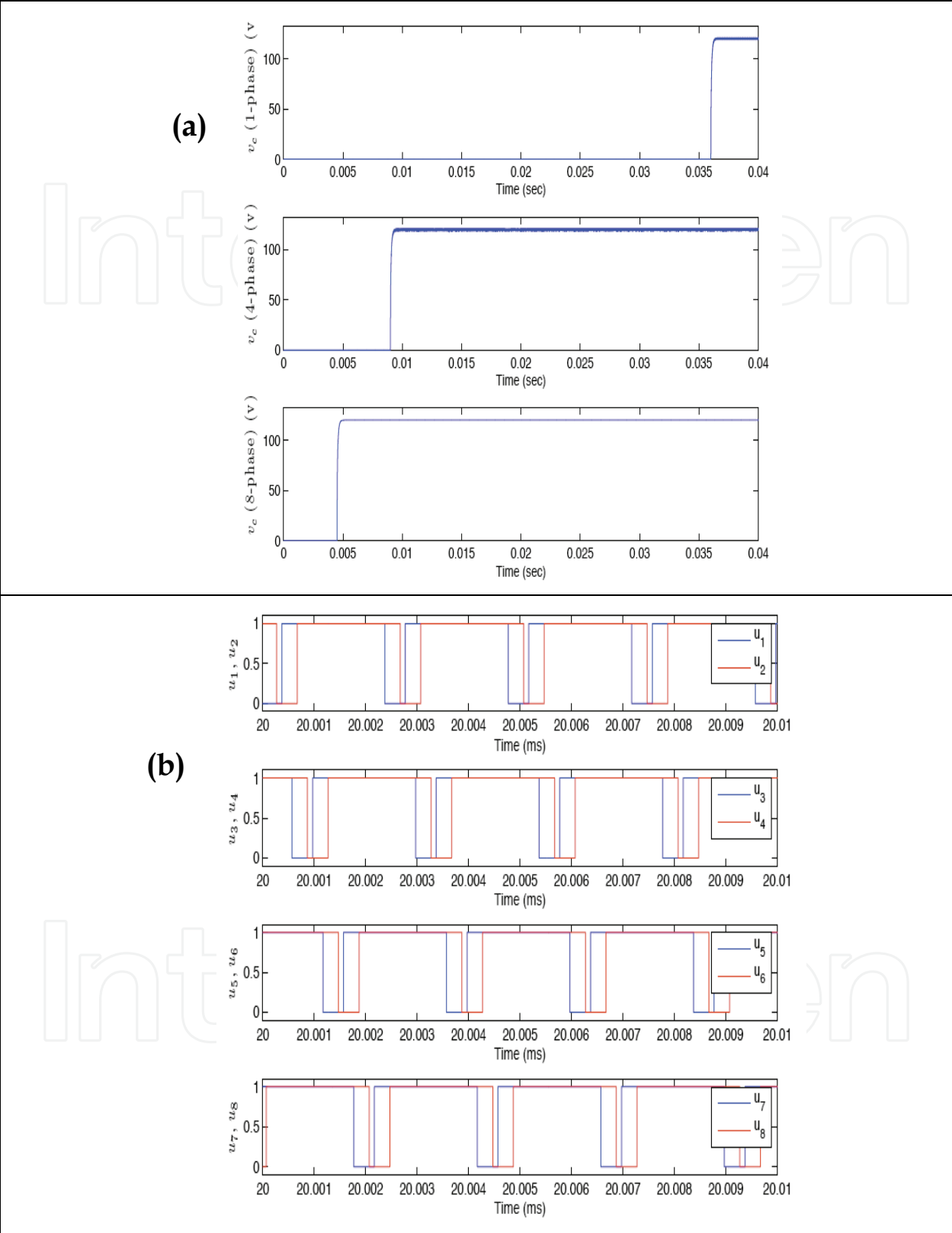desired phase shift of one quarter chattering period is provided.

Fig. 23. Simulation of 1-phase, 4-phases and 8-phases Boost converter with $v_{sp} = 120\text{V}$. Figure (b) shows the switching command for the case of 8-phase boost converter. Clearly, a desired phase shift of one-eighth chattering period is provided.

The needed gain $K_h = 1/\alpha$ in figure 13 to implement a hysteresis loop of width $\alpha\Delta$ is calculated based on equation (66), i.e.,

$$\alpha = \frac{1}{K_h} = \begin{cases} \dfrac{4b^2}{n(b^2 - a^2)} & \text{if } \left|\dfrac{a}{b}\right| < \left(1 - \dfrac{2}{n}\right) \\[3mm] \dfrac{2b}{b + |a|} & \text{if } \left(1 - \dfrac{2}{n}\right) \leq \left|\dfrac{a}{b}\right| < 1 \end{cases} \tag{92}$$

In figures 28-31, several simulations are conducted with converter's parameters:

$E = 20\text{V}$, $L = 40mH$, $C = 4\mu F$.

In the simulation in figure 28-29, the output voltage converges more rapidly to the desired set point voltage $v_{sp} = 40\text{V}$ for the case of 4-phases compared to the 2-phase and 1-phase cases. This is because of the fact that for a 4-phase power converter, only one fourth of the total current needed is tracked in each phase leg resulting in a faster convergence. It is also evident that a desired phase shift of $T/4$ is successfully provided with the switching frequency controlled to be $f = 1/T \approx 40\text{KHz}$. In simulations shown in figures 30-31, 4-phases is not enough to suppress chattering and thus eight phases is used to provide harmonics cancellation (for up to the seven harmonic) resulting in an acceptable level of chattering. The output voltage converges to the desired voltage $v_{sp} = 120\text{V}$ at a much faster rate than that for the 1-phase and 4-phases cases for the same reason mentioned earlier.

## 8. Conclusion

Sliding Mode Control is one of the most promising techniques in controlling power converters due to its simplicity and low sensitivity to disturbances and parameters' variations. In addition, the binary nature of sliding mode control makes it the perfect choice when dealing with modern power converters with "ON/OFF" as the only possible operation mode. In this paper, how the widely used PID controller can be easily implemented by enforcing sliding mode in the power converter. An obstacle in implementing sliding mode is the presence of finite amplitude and frequency oscillations called chattering. There are many factors causing chattering including imperfection in switching devices, the presence of unmodeled dynamics, effect of discrete time implementations, etc.
In this chapter, a method for chattering reduction based on the nature of sliding mode is presented. Following this method, frequency of chattering is first controlled to be equal to the maximum allowable value (corresponding to the maximum allowable heat loss) resulting in the minimum possible chattering level. Chattering is then reduced by providing a desired phase shift in a multiphase power converter structure that leads to harmonics elimination (and thus chattering reduction) at the output. The outlined theory is then applied in designing multiphase DC-DC buck and boost converters.

# 9. References

Al-Hosani, K., & Utkin, V. I. (2009). Multiphase power boost converters with sliding mode. *Multi-conference on Systems and Control* (pp. 1541-1544 ). Saint Petersburg, RUSSIA: IEEE.

Al-Hosani, K., Malinin, A. M., & Utkin, V. I. (2009). Sliding Mode PID Control and Estimation for Buck Converters. *International Conference on Electrical Drives and Power Electronics.* Dubrovnik, Croatia.

Al-Hosani, K., Malinin, A. M., & Utkin, V. I. (2009). Sliding mode PID control of buck converters. *European Control Conference.* Budapest, Hungary.

Bondarev, A. G., Bondarev, S. A., Kostyleva, N. E., & Utkin, V. I. (1985). Sliding Modes in Systems with Asymptotic Observer. *Automation Remote Control , 46,* 49-64.

Bose, B. K. (2006). *Power Electronics And Motor Drives: Advances and Trends* (1st Edition ed.). Academic Press.

Cortes, D., & Alvarez, J. (2002). Robust sliding mode control for the boost converter. *Power Electronics Congress, Technical Proceedings, Cooperative Education and Internship Program, VIII IEEE International* (pp. 208-212). Guadalajara, Mexico.

Emelyanov, S., Utkin, V. I., Taran, V., Kostyleva, N., Shubladze, A., Ezerov, V., et al. (1970). *Theory of Variable Structutre System.* Moscow: Nauka.

Lee, H. (2007). *PhD Thesis, Chattering Suppresion in Sliding Mode Control System.* Columbus, OH, USA: Ohio State University.

Lee, H., & Utkin, V. I. (2006). Chattering Analysis. In C. Edwards, E. C. Colet, & L. Fridman, *Advances in Variable Structure and Sliding Mode Control* (pp. 107-121). London.

Lee, H., & Utkin, V. I. (2006). The Chattering Analysis. *12th International Power Electronics and Motion Control Conference* (pp. 2014-2019). Portoroz, Slovenia: IEEE.

Lee, H., Uktin, V. I., & Malinin, A. (2009). Chattering reduction using multiphase sliding mode control . *International Journal of Control , 82* (9), 1720-1737.

Miwa, B., Wen, D., & Schecht, M. (1992). High Effciency Power Factor Correction Using Interleaving Techniques. *IEEE Applied Power Electronics Conference.* Boston, MA: IEEE.

Mohan, N., Undeland, T. M., & Robbins, W. P. (2003). *Power Electronics: Converters, Applications, and Designs* (3rd Edition ed.). John Wiley & Sons, Inc.

Nguyen, V., & Lee, C. (1995). Tracking control of buck converter using sliding-mode with adaptive hysteresis. *Power Electronics Specialists Conference, 26th Annual IEEE. 2,* pp. 1086 - 1093. Atlanta, GA: IEEE.

Sira-Ramírez, H. (2006). *Control Design Techniques in Power Electronics Devices.* Springer.

Slotine, J.-J. (1984). Sliding Controller Design for Nonlinear Systems. *International Journal of Control , 40* (2), 421-434.

Slotine, J.-J., & Sastry, S. S. (1983). Tracking Control of Nonlinear Systems using Sliding Surfaces, with Application to Robot Manipulator. *International Journal of Control , 38* (2), 465-492.

Utkin, V., Guldner, J., & Shi, J. (2009). *Sliding Mode Control in Electro-Mechanical Systems.* CRC Press, Taylor & Francis Group.

Wu, W., Lee, N.-C., & Schuellein, G. (2006). Multi-phase buck converter design with two-phase coupled inductors. *Applied Power Electronics Conference and Exposition, Twenty-First Annual IEEE* (p. 6). Seattle, WA: IEEE.

Xu, P., Wei, J., & Lee, F. (2003). Multiphase coupled-buck converter-a novel high efficient 12 V voltage regulator module. *IEEE Transactions on Power Electronics , 18* (1), 74-82.
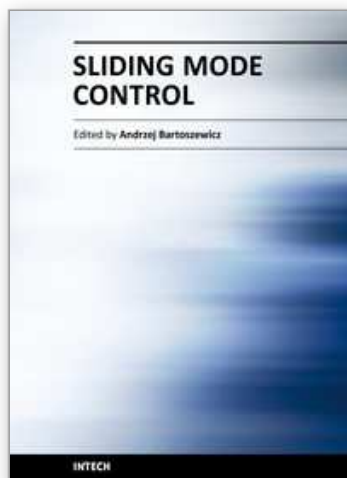
**Sliding Mode Control**

Edited by Prof. Andrzej Bartoszewicz

The main objective of this monograph is to present a broad range of well worked out, recent application studies as well as theoretical contributions in the field of sliding mode control system analysis and design. The contributions presented here include new theoretical developments as well as successful applications of variable structure controllers primarily in the field of power electronics, electric drives and motion steering systems. They enrich the current state of the art, and motivate and encourage new ideas and solutions in the sliding mode control area.

**How to reference**

In order to correctly reference this scholarly work, feel free to copy and paste the following:

# INTECH
open science | open minds